Journal Pre-proof

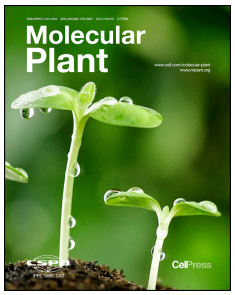

Enhanced Vitamin C Production Mediated by an ABA-Induced PTP-Like Nucleotidase Improves Drought Tolerance of Arabidopsis and Maize

Hui Zhang, Yanli Xiang, Neng He, Xiangguo Liu, Hongbo Liu, Liping Fang, Fei Zhang, Xiaopeng Sun, Delin Zhang, Xingwang Li, William Terzaghi, Jianbing Yan, Mingqiu Dai

PII: S1674-2052(20)30035-6
DOI: https://doi.org/10.1016/j.molp.2020.02.005
Reference: MOLP 893

To appear in: *MOLECULAR PLANT*
Accepted Date: 10 February 2020

Please cite this article as: **Zhang H., Xiang Y., He N., Liu X., Liu H., Fang L., Zhang F., Sun X., Zhang D., Li X., Terzaghi W., Yan J., and Dai M.** (2020). Enhanced Vitamin C Production Mediated by an ABA-Induced PTP-Like Nucleotidase Improves Drought Tolerance of Arabidopsis and Maize. Mol. Plant. doi: https://doi.org/10.1016/j.molp.2020.02.005.

This is a PDF file of an article that has undergone enhancements after acceptance, such as the addition of a cover page and metadata, and formatting for readability, but it is not yet the definitive version of record. This version will undergo additional copyediting, typesetting and review before it is published in its final form, but we are providing this version to give early visibility of the article. Please note that, during the production process, errors may be discovered which could affect the content, and all legal disclaimers that apply to the journal pertain.

All studies published in MOLECULAR PLANT are embargoed until 3PM ET of the day they are published as corrected proofs on-line. Studies cannot be publicized as accepted manuscripts or uncorrected proofs.

© 2020 The Author

Journal Pre-proof

Enhanced Vitamin C Production Mediated by an ABA-Induced PTP-Like Nucleotidase Improves Drought Tolerance of Arabidopsis and Maize

Hui Zhang[1a], Yanli Xiang[1a], Neng He[1], Xiangguo Liu[2], Hongbo Liu[1], Liping Fang[1], Fei Zhang[1], Xiaopeng Sun[1], Delin Zhang[1], Xingwang Li[1], William Terzaghi[3], Jianbing Yan[1] and Mingqiu Dai[1b]

[1]National Key Laboratory of Crop Genetic Improvement, Huazhong Agricultural University, Wuhan 430070, China

[2]Jilin Provincial Key Laboratory of Agricultural Biotechnology, Agro□Biotechnology Institute, Jilin Academy of Agricultural Sciences, Changchun 130124, China

[3] Department of Biology, Wilkes University, Wilkes-Barre, Pennsylvania 18766

[a] These authors contributed equally to this article.

[b] Corresponding author: mingqiudai@mail.hzau.edu.cn

Short Summary: How ABA and vitamin C signaling pathways interact in stress responses remains elusive. In this study, we demonstrate that PTPN has nucleotidase activity. *PTPN* is activated by ABA signaling pathway and is a key regulator of drought-promoted vitamin C production, thus mediated the crosstalk between ABA signaling and vitamin C biosynthesis pathways and positively regulate plant drought tolerance.

Journal Pre-proof

Journal Pre-proof

ABSTRACT

Abscisic acid (ABA) is a key phytohormone that mediates environmental stress responses. Vitamin C, or L-ascorbic acid (AsA), is the most abundant antioxidant against stress damages in plant. How ABA and AsA signaling pathways interact in stress responses remains elusive. In this study, we characterized a previously unidentified gene, *PTPN* (*PTP-like Nucleotidase*). Arabidopsis *PTPN* (*AtPTPN*) was expressed in multiple tissues and upregulated by ABA and drought treatments. *Atptpn* mutants were hyposensitive to ABA but hypersensitive to drought stresses, while plants with enhanced expression of *AtPTPN* showed opposite phenotypes to *Atptpn*. Overexpressing maize *PTPN* (*ZmPTPN*) promoted, while knock-down *ZmPTPN* inhibited plant drought tolerance, indicating conserved and positive roles of *PTPN* in plant drought tolerance. AtPTPN and ZmPTPN released Pi by hydrolyzing GDP/GMP/dGMP/IMP/dIMP. AtPTPN positively regulated AsA production via endogenous Pi contents control. Overexpression of VTC2, the rate-limiting synthetic enzyme in AsA biosynthesis, promoted AsA production and plant drought tolerance, which is largely dependent of AtPTPN activity. We further demonstrated that the heat shock transcription factor HSFA6a directly bound *AtPTPN* promoter and activated *AtPTPN* expression. Genetic interaction assays showed that *AtPTPN* was required for *HSFA6a* to regulate ABA and drought responses. Our data indicate a PTPN-mediated crosstalk between ABA signaling and AsA biosynthesis pathways that positively control plant drought tolerance.

Keywords: Nucleotidase, Abscisic acid, Vitamin C, Drought, Arabidopsis, Maize

Journal Pre-proof

INTRODUCTION

Higher plants are sessile organisms, which suffer from various kinds of stresses throughout their lives. Drought is one of the major abiotic stresses that negatively affect plant growth and development, therefore higher plants have evolved sophisticated mechanisms to respond to drought. The phytohormone abscisic acid (ABA) is important for plant drought responses. During drought stress, plants increase the production of ABA, which functions as a signal resulting in the closure of stomatal guard cells to prevent water loss (Himmelbach et al., 2003). Recently, a number of regulators mediating ABA signaling have been identified. Two different groups have reported that PYL/RCAR proteins are ABA receptors (Ma et al., 2009; Park et al., 2009). The clade A PP2C phosphatases and SnRK2 kinases have also been shown to be important in ABA signaling (Raghavendra et al., 2010). A number of studies have revealed the critical roles of PYL/RCAR ABA receptors, clade A PP2C phosphatases and SnRK2 kinases in regulation of plant drought responses (Fujii and Zhu, 2009; Zhao et al., 2016; Xiang et al., 2017; He et al., 2018). The ABF/AREB (abscisic acid-responsive element binding factor) transcription factors (TFs) are downstream regulators of ABA signaling. Under drought stress, ABFs are phosphorylated and activated by SnRK2 kinases, which in turn regulate gene expression and drought responses (Yoshida et al., 2010; Fujita et al., 2013).

Another family of TFs involved in environmental stress-responses are heat shock factors (HSFs) (von Koskull-Döring et al., 2007; Ohama et al., 2017). Twenty-one HSF TFs have been identified in the Arabidopsis genome and have been placed in three major classes (A-C) (Nover et al. 2001). A genome-wide survey of HsfA1a binding sites has been conducted. In addition to the perfect heat shock element (nTTCnnGAAnnTTCn), three novel types of binding sites have been found: Gap-type, TTC-rich and stress response element (STRE) (Guo et al., 2008), suggesting extensive roles of HsfA TFs in regulation of gene expression. The HsfA TFs play critical roles in plant drought tolerance. Tomato HsfA1 positively regulates plant drought tolerance by activating ATG genes and inducing autophagy (Wang et al., 2015). Over-expression of

Journal Pre-proof

HsfA6a in Arabidopsis promoted ABA sensitivity and enhanced drought tolerance, suggesting a positive role of HsfA6a in drought response (Hwang et al., 2014). Three ABA response elements (ABRE) were identified in the promoter region of *HsfA6a*. Multiple experiments proved that ABF transcription factors, such as ABF2, ABF3, and ABF4 bound these ABREs, indicating that HsfA6a functions in drought responses via the ABA-dependent signaling pathway (Hwang et al., 2014). However, the downstream targets of HsfA6a in plant drought response remain elusive.

Drought promotes the production of reactive oxygen species (ROS), such as H_2O_2, singlet oxygen and superoxide anion radical (O^{2-}), which cause oxidative signaling (Choudhury et al., 2017). Beyond their basal levels, ROS cause oxidative stress and are toxic to the cells (Mittler, 2017). Vitamin C, or L-ascorbic acid (AsA), is the maximum antioxidant in plants that protects cells against oxidative stress caused by ROS (Gallie, 2013; Akram et al., 2017). In plants, AsA is mainly synthesized via the Smirnoff-Wheeler pathway, initiating from D-mannose-1-P and comprising the sequential conversion of GDP-D-mannose into GDP-L-galactose, L-galactose-1-P, L-galactose, L-galactono-1,4-lactone and L-ascorbate (Wheeler et al., 1998; Valpuesta and Botella, 2004). Several key enzymes have been identified that catalyze the biosynthetic steps in the Smirnoff-Wheeler pathway, such as VTC1, GME, VTC2, VTC4 and VTC5 (Wheeler et al., 1998; Conklin et al., 1999; Conklin et al.,2000; Conklin et al., 2006; Dowdle et al., 2007). VTC2 has been identified as a rate-limiting enzyme in AsA biosynthesis (Yoshimura et al., 2014). The homologs of all these Smirnoff-Wheeler pathway enzymes have been found in other plants, such as tomato, acerola, kiwifruit and even in algal species (Badejo et al., 2009; Bulley et al., 2009; Ioannidi et al., 2009; Urzica et al., 2012), indicating a conserved plant AsA biosynthetic pathway. It has been revealed that VTC2 and VTC5 are highly specific for and dependent on phosphate (Pi) for conversion of GDP-L-galactose into L-galactose-1-P (Linster et al., 2007). While the enzymes catalyzing AsA biosynthesis have been widely studied, knowledge about the regulation of AsA production in response to environmental stresses is limited.

In this study, we characterized a previously unidentified gene, *PTPN* (for *PTP-like Nulceotidase*). Mutation of *AtPTPN* by T-DNA insertion and Crispr editing decreased

plant sensitivities to ABA but increased their sensitivities to drought and osmotic stresses. In contrast, plants with enhanced expression of *AtPTPN* were more sensitive to ABA, but more tolerant to drought. Overexpression *PTPN* of maize (*ZmPTPN*) enhanced， while knock-down *ZmPTPN* inhibited plant drought tolerance. These observations indicated positive and conserved roles of PTPN in drought responses of Arabidopsis and maize. *PTPN* encodes an enzyme with nucleotidase activity that is required to regulate AsA biosynthesis. We show that *AtPTPN* expression is up-regulated by drought and ABA treatments, and that HsfA6a directly binds *AtPTPN* promoter and activates the expression of *AtPTPN*. Our findings suggest that AtPTPN could be a nexus in mediating ABA signaling and AsA biosynthesis pathways that positively regulate plant drought tolerance.

RESULTS

AtPTPN Loss-of-function mutants were hyposensitive to ABA

ABA promotes the closure of stomatal guard cells and prevents water loss under drought (Himmelbach et al., 2003), therefore is important for plant drought responses. Protein phosphorylation, which is regulated by protein phosphatases and kinases, has been revealed important for ABA signaling (Fujita et al., 2013). We screened the ABA sensitivities of ~140 T-DNA insertion mutants of genes encoding Arabidopsis phosphatases with unknown function. Of these mutants, SALK_023939 was chosen for further analysis based on its phenotypes responding to ABA. In the SALK_023939 mutant, the T-DNA was inserted into the eleventh exon of AT3G62010 resulting in a knock-out mutation (*Atptpn-1*) (Supplemental Figure 1A-C). We further generated a knock-out mutant allele of AT3G62010 (*Atptpn-2*) via Crispr/Cas9 system, which had a deletion of 101 bp in the first exon of AT3G62010 (Supplemental Figure 1D and E). The genomic sequence of AT3G62010 has 19 exons. The open reading frame (3762 nt) encodes a protein of 1254 amino acids. According to the National Center for Biotechnology Information (NCBI) protein database, AT3G62010 encodes a PTP-like phosphatase, therefore we named this gene *AtPTPN* (*PTP-like Phosphatase*). A

Journal Pre-proof

protein BLAST search of the NCBI protein database discovered PTPN homologs in higher plants, including dicots and monocots, and even in fungi (*Schizophyllum commune*) (Supplemental Figure 2). In higher plants, the sequence identities of PTPN homologs ranged from 88% (monocots) to ~94% (dicots). The full-length AtPTPN protein apparently has three repeated regions (PTPNa-c), with 46%, 34% and 30% identities between a/b, a/c and b/c respectively (Supplemental Figure 3A). This feature is conserved in all PTPN homologs across various species (Supplemental Figure 3B). Together, these data suggested evolutionary conservation of PTPN.

When grown on MS plates with ABA at various concentrations, the proportions of green cotyledons in *Atptpn-1* and *Atptpn-2* mutants were significantly higher than those of wild type (Figure 1A and B). We also measured the stomatal apertures of 10-day-old wild type, *Atptpn-1* and *Atptpn-2* leaves in response to ABA, and observed that stomata of *Atptpn-1* and *Atptpn-2* mutants closed more slowly than wild type under ABA treatment (Figure 1C and D). Taken together, these data indicate that *AtPTPN* is a negative regulator of ABA responses.

PTPN mutants were sensitive, while plants with enhanced _PTPN_ expression were tolerant to drought

The ABA hyposensitivity of stomatal closure in *AtPTPN* mutants implied that *AtPTPN* may have roles in plant drought responses. To test this hypothesis, we stopped irrigation of 4-week-old wild type, *Atptpn-1* and *Atptpn-2* mutant plants for ~16 days and then rewatered. Their survival rates were scored 3 days after rewatering. We observed significantly lower survival rates in *Atptpn-1* and *Atptpn-2* mutants (~38% on average) as compared with wild type (~70% on average) (Figure 1E and F). In addition, detached *Atptpn-1* and *Atptpn-2* leaves lost water much faster than wild type (Figure 1G). These results indicated that *Atptpn-1* and *Atptpn-2* mutants were more sensitive to drought stress. We also observed that *Atptpn-1* mutants were more sensitive to mannitol treatment, which causes osmotic stress (Supplemental Figure S4). Proline is an osmolyte that protects plants from drought stress (Yoshiba et a., 1997). Drought-induced ROS promotes increased content of malondialdehyde (MDA). MDA is

a product caused by lipid peroxidation, and its level is an indicator of oxidative damage that is widely used to differentiate sensitivity or tolerance of plants to stresses (Hernández et al, 2000; Shalata et al., 2001; Yu et a., 2017). We investigated the production of proline and MDA in wild type plants, *Atptpn-1* and *Atptpn-2* mutants grown in drought and well-watered conditions. The results showed that the *Atptpn-1* and *Atptpn-2* mutants produced less proline, but more MDA than wild type plants after drought stress; while under well-watered conditions, there were no differences in production of proline or MDA in wild type, *Atptpn-1* and *Atptpn-2* mutant plants (Figure 1H and I). In addition, *Atptpn-1* and *Atptpn-2* mutants produced more H_2O_2 contents than wild type plants after drought stress (Figure 1J).

ABA is a key stress hormone and important for plant drought tolerance. We investigated the ABA contents in wild type, *Atptpn-1* and *Atptpn-2* mutants. The results showed that drought promoted the production of ABA in all plants, but the elevated ABA levels in both *Atptpn-1* and *Atptpn-2* mutant plants were significantly lower than those of wild type plants after drought stress (Figure 1K). Additionally, the induced expression levels of ABA responsive genes (*ABI2*, *ABF3* and *RD29B*) in *Atptpn-1* and *Atptpn-2* mutant plants were lower than those in Col-0 plants after ABA treatment (Figure 1L). These results indicate reduced ABA production in *Atptpn-1* and *Atptpn-2* mutants after drought stress, and impaired ABA signaling in these mutants.

Next, we expressed *AtPTPN (*35S::*AtPTPN-3HA)* in *Atptpn-1* mutants via transgenic approaches, and observed that the *Atptpn-1* mutants were recovered with ABA and drought phenotypes by the transgene (Supplemental Figure S5). We further expressed 35S::*AtPTPN-3HA* in Col-0 wild type background to generate *AtPTPN* enhanced transgenic plants (OE-5, OE-6, Figure S6A and B). When grown on MS plates with ABA at various concentrations, the proportions of green cotyledons in OE-5 and OE-6 plants were significantly lower than those of Col-0 (Figure S6C and D). We stopped irrigation of 4-week-old soil-grown wild type, OE-5 and OE-6 plants and then rewatered when these plants showed severe stress symptoms. Their survival rates were scored 3 days after rewatering. We observed significantly higher survival rates of OE-5 and OE-6 plants (~80% on average) as compared with wild type (~20% on

Journal Pre-proof

average) (Figure S6E and F). After drought stress, OE-5 and OE-6 plants produced more proline, but less MDA and H_2O_2 than wild type plants; while under well-watered conditions, there were no differences in production of these molecules in wild type and transgenic plants (Figure S6G, H and I). Together, these observations suggested that *AtPTPN* play positive roles in plant drought tolerance, may through reducing the oxidation damage caused by drought.

Maize is an important crop worldwide. There is one gene, GRMZM2G146819, that encodes a maize AtPTPN homolog ZmPTPN (Supplemental Figure S2). We overexpressed *ZmPTPN* in maize and observed that plants overexpressing *ZmPTPN* were more tolerant to drought, as revealed by higher survival rates of the positive transgenic maize plants after drought stress compared to those of their negative siblings (Supplemental Figure S7). In contrast, *ZmPTPN* knock-down plants were more sensitive to drought (Supplemental Figure S8). These studies indicate a positive and conserved role of *PTPN* in regulation of plant drought tolerance.

Temporal/spatial and stress-responsive expression of *AtPTPN*

In order to determine the temporal and spatial expression patterns of *AtPTPN,* we generated transgenic Arabidopsis plants harboring the *AtPTPNp*::*GUS* transgene. GUS staining assays were performed and the staining signals were detected in roots, cotyledons, hypocotyls, guard cells, and floral organs, such as ovule, filaments, pistils, and pollen in the transgenic plants, indicating the expression of *AtPTPN* in these tissues (Figure 2A). The expression of *AtPTPN* in multiple tissues suggested possible roles of this gene in plant development.

To determine how *AtPTPN* responded to ABA and drought treatments, two-week-old seedlings of wild type were subjected to exogenous ABA and drought treatments, then the roots and shoots were harvested separately after various levels of stresses. RT-qPCR analyses showed that in both roots and shoots, ABA strongly promoted the expression of *AtPTPN*. An increase in *AtPTPN* expression was detected after one hour of ABA treatment, and the *AtPTPN* expression was higher after 3 hours of ABA treatment and continued to increase following continued ABA exposure (Figure

2B and C). *AtPTPN* expression was also induced by drought stress, and the induction patterns were similar to those after ABA treatment (Figure 2D and E). SNF1-related protein kinase subfamily 2 (SnRK2s) encoding genes, including *SnRK2.2*, *SnRK2.3* and *OST1* (or *SnRK2.6*) are key regulators of ABA signaling pathway and important for plant drought tolerance (Fuiji and Zhu, 2009). After drought, *AtPTPN* expression was promoted, but this expression pattern of *AtPTPN* in response to drought was abolished in *ost1* (*snrk2.6*) and *snrk2.2*/*2*/*3*/*6* mutants (Supplemental Figure S9), indicating that response of *AtPTPN* to drought is dependent on ABA signaling. Together, these observations suggested that *AtPTPN* functions in drought and ABA responses, which is consistent with the results of the functional studies (Figure 1 and 2).

We further investigated the subcellular localization of AtPTPN by transient expression of 35S:*GFP-AtPTPN*, 35S:*GFP* (as a control) and HY5-RFP (nucleus localized) in the mesophyll protoplast cells extracted from Arabidopsis leaves. We observed that GFP-AtPTPN and GFP showed very similar subcellular localization in the protoplasts (Figure 2F). To exclude the possibility that this localization pattern of GFP-AtPTPN was due to the degradation of AtPTPN or failure of *AtPTPN* expression, we extracted the proteins from the protoplasts and performed western blot assays. The results showed that both GFP-AtPTPN and GFP were successfully expressed in the protoplasts transformed with 35S:*GFP-AtPTPN* or 35S:*GFP* respectively (Figure 2G). It has been reported that the GFP signal is localized in the cytoplasm of Arabidopsis mesophyll protoplasts (Ding et al., 2015). Therefore, AtPTPN could be also localized in the cytoplasm, but not in the nucleus (Figure 2F and H).

PTPN **encodes an enzyme with nucleotidase activity**

We next sought to identify the substrates of PTPN. Bioinformatics analyses showed that AtPTPNa and AtPTPNb contained NCxxGxxRT motifs (x is for any amino acid) (Supplemental Figure S3), which were very similar to the previously identified P loop of phytase consisting the catalytically important HCxxGxxR(T/S) sequence motif in hydrolyzing phytic acid (Chu et al., 2004). We therefore expressed AtPTPN in insect cells and purified the target protein to assay *in vitro* phosphatase activity. Interestingly,

we did not observe any phytate hydrolysis by AtPTPN (Supplemental Figure S10A), indicating that the AtPTPN NCxxGxxRT motifs did not have phytase activity. To identify its substrates, we next tested AtPTPN with 49 chemicals *in vitro* activity assays (Supplemental Table 1). We found that AtPTPN hydrolyzed GMP, dGMP, GDP, IMP, and dIMP (Figure 3A; Supplemental Figure S10B). These results indicated that AtPTPN is an enzyme with nucleotidase activity.

Temperature, pH and divalent metal ion concentrations are important factors affecting the activity of an enzyme. To identify the AtPTPN optimum temperature, we performed activity assays with GMP and dGMP as substrates. The results showed that AtPTPN had strongest activity at 30 ℃, while it was inactivated by 45℃ or higher temperatures (in a range of 20-50 ℃) (Figure 3B). We next determined the AtPTPN pH optimum using GMP and dGMP and found that at 30 ℃, pH 5 was optimal for AtPTPN activity toward these substrates (Figure 3C). Interestingly, another AtPTPN activity peak was observed at pH 3 while pH of 4.5 almost inactivated AtPTPN, similar to what pH of 8 did to this enzyme (Figure 3C). Further, at 30 ℃ and pH 5, we observed that Ca^{2+}, Mg^{2+} and Mn^{2+} activated while Cu^{2+} killed the AtPTPN activity on GMP (Figure 3D). The optimal Ca^{2+} concentration was 0.5 mM, while there were broad concentration optima of Mg^{2+} and Mn^{2+} for AtPTPN activity (0.5-10 mM) (Figure 3D). These results suggested that Ca^{2+}, Mg^{2+} and Mn^{2+} were activators, while Cu^{2+} was an inhibitor of AtPTPN.

The ZmPTPN and AtPTPN sequence identity is 72%, indicating high conservation of PTPN sequence between maize and Arabidopsis (Supplemental Figure S2). To determine whether PTPN activity was conserved among plants, we did the same substrate screening experiments for ZmPTPN. Among these substrates, we found that ZmPTPN hydrolyzed GMP, dGMP, GDP, IMP and dIMP (Figure 3E, Supplemental Figure S10C). Further experiments showed that ZmPTPN had a broad temperature optimum (20-35℃) and pH optimum (3-7) towards GMP and dGMP (Figure 3F and G). Similar to AtPTPN, ZmPTPN was activated by Ca^{2+}, Mg^{2+} and Mn^{2+}, but inhibited by Cu^{2+} (Figure 3H). These results indicated a conservation of enzyme activity between ZmPTPN and AtPTPN.

Journal Pre-proof

AtPTPN activity is required for AsA biosynthesis

AsA is the major plant antioxidant and protects cells by detoxification of oxidation generated by various stresses (Gallie, 2013; Akram et al., 2017). The AsA biosynthesis pathway, the Smirnoff-Wheeler pathway, has been widely studied in plants (Wheeler et al., 1998; Valpuesta and Botella, 2004). A summary of the Smirnoff-Wheeler pathway is shown in Figure 4A. Pi has been reported to play a critical role in converting GDP-L-Galactose into L-Galactose-1-P by VTC2 and VTC5, a rate-limiting step in AsA biosynthesis (Yoshimura et al., 2014). There is no VTC2 or VTC5 activities in the absence of Pi (Yoshimura et al., 2014). Given that AtPTPN hydrolyzed GDP/GMP/dGMP/IMP/dIMP to release Pi (Figure 3), we hypothesized that the endogenous Pi generated by AtPTPN would play a role in AsA biosynthesis. To test this hypothesis, we first investigated the AsA contents of *Atptpn-1* and wild type plants treated with or without drought stress. The results showed that there were reduced amounts of total AsA in *Atptpn-1* mutants as compared to wild type plants (Figure 4B). We also observed a reduction of total AsA in *Atptpn-1* mutants and wild type plants after drought stress as compared to those plants without drought stress (Figure 4B), which was consistent with the knowledge that water stress results in the depletion of the AsA pool (Smirnoff and Pallanca, 1996; Leung and Giraudat, 1998; Pastori and Foyer, 2002). In consistent with the decreased AsA levels, the endogenous Pi contents in *Atptpn-1* mutants were also significantly reduced as compared to those in wild type plants (Figure 4C). When exogenous Pi ($HPO4^{2-}$) was supplied to *Atptpn-1* mutants, we observed that the AsA production was recovered in these mutants (Supplemental Figure S11).

We next checked the expression of several key genes encoding AsA biosynthetic enzymes VTC1, VTC2, VTC4 and VTC5, according to the Smirnoff-Wheeler pathway (Figure 5A). The results showed that the expression levels of these *VTC* genes were down-regulated in *Atptpn-1* mutants as compared to wild type plants after drought stress (Figure4D).

How VTC2, the rate-limiting enzymes in AsA biosynthesis (Yoshimura et al., 2014), regulates plant drought response remains unknown. To know the roles of *VTC*2 in drought response and its interaction with *PTPN*, we overexpressed this gene in wild type (35S::*VTC2-3HA*/Col-0, or *VTC2*/C) and *Atptpn-1* mutants (35S::*VTC2-3HA*/*Atptpn-1*, or *VTC2*/*p*) (Figure 4E). We measured the AsA contents in the transgenic lines. The results showed that the AsA contents in *VTC2*/*p* plants were significantly lower than those in *VTC2*/C plants (Figure 4F). We also observed that the survival rates of *VTC2*/*p* plants were significantly lower than those in *VTC2*/C plants after drought stress (Figure 4G), demonstrating that VTC2 has a positive role in drought tolerance. These results also indicated that the function of VTC2 in AsA biosynthesis and drought tolerance might depend on AtPTPN activity.

HSFA6a directly binds the *AtPTPN* promoter and activates *AtPTPN* expression

We next asked which TFs regulate *AtPTPN* expression in response to drought. To answer this question, a yeast one-hybrid (Y1H) screening of TFs binding the *AtPTPN* promoter was conducted using a previously-reported library of 1589 Arabidopsis TFs (Ou et al., 2011). The promoter region of the *AtPTPN* gene (-1974 to 1) was dissected into 4 fragments (P1-P4) (Figure 5A), and these truncated mini promoters were expressed with the TFs in yeast cells. We found a TF, HSFA6a, that interacted with the P4 fragment in yeast cells (Figure 5B and C). HSFA6a is a heat shock transcription factor classified as a member of subfamily A and plays important roles in plant drought tolerance (Hwang et al., 2014). A previous study has reported that HSFA1a, another member of HSF subfamily A, binds a TTC-rich element nTTCnnnnnTTCn (n is any nucleotide) (Guo et al., 2008). Sequence analysis revealed a TTC-rich element (TTTCCGGGATTCG) in the P4 fragment (Figure 5A). To determine whether HSFA6a could bind this element (HSE, heat shock factor binding element), an electrophoretic mobility shift assay (EMSA) was performed. The results showed that GST-HSFA6a bound to the biotin-labeled HSE (Biotin-HSE), but not the biotin-labeled HSEmu, a mutation to HSE (Figure 5A), to form complexes that migrated more slowly on the gel, and these complexes vanished after adding unlabeled HSE probes (Figure 5D). As a

negative control, GST did not bind to Biotin-HSE nor Biotin-HSEmu (Figure 5D). These results indicated that HSFA6a directly bound to the HSE in the P4 promoter fragment.

To ascertain whether HSFA6a could interact with P4 fragment *in vivo*, *HSFA6a* was co-expressed (*35S*::*HSFA6a*) with the reporter (*P4*::*LUC*) in Arabidopsis protoplasts, and the relative luciferase (LUC) activity was measured. The results showed that expression of HSFA6a, as compared with the empty pRTL2, more greatly enhanced the expression of *LUC* in protoplasts (Figure 4E), implying the interaction of HSFA6a with the P4 mini promoter *in vivo*. To test whether HSFA6a bind to HSE element of P4 in plant, we performed chromatin immunoprecipitation with quantitative PCR (ChIP-qPCR) using DNA extracted from the *HSFA6a*-OE transgenic plants (35S::*HSFA6a-3HA*/Col-0) and Col-0 wild type. Indeed, the fragment containing HSE was enriched to significantly higher levels in DNA from *HSFA6a*-OE transgenic plants as compared to Col-0 DNA precipitated with HA antibody (Figure 5F). As a negative control, the fragment in P4 without HSE did not show significant difference of enrichment between DNA samples from *HSFA6a*-OE transgenic plants and Col-0 (Figure 5F). These results indicated that HSFA6a directly associated with *AtPTPN* promoter at HSE in vivo.

Genetic interactions between *AtPTPN* and *HSFA6a* in ABA and drought responses

To learn how *AtPTPN* and *HSFA6a* genetically interact, we overexpressed *HSFA6a* in the *Atptpn-1* mutant (*35S*::*HSFA6a-3HA*/*Atptpn-1,* or *HSFA 6a-OE/*p) and wild type (*35S*::*HSFA6a-3HA*/Col-0*, or HSFA6a-OE*/C) backgrounds. Two independent transgenic lines overproducing *HSFA6a-3HA* from each background were chosen in the assays (Figure 6A). In the wild type background, overexpression of *HSFA6a* slightly enhanced the expression of *AtPTPN* (~1.5 folds) under normal growth conditions, but more strongly (~2.5 folds) under drought stresses (Figure 6B), indicating that drought promoted the transcriptional activity of HSFA6a, and that *AtPTPN* is a target of HSFA6a activity. When treated with ABA at concentrations of 0.5, 0.75 or 1.0 μM, the cotyledons of *HSFA6a-OE/*C lines were not as green as those of wild type (Figure 6C and D), suggesting hypersensitivity of *HSFA6a-OE/*C lines to ABA, consistent with a previous

Journal Pre-proof

report (Hwang et al., 2014). In the *Atptpn-1* mutant background, the ABA-hypersensitive phenotypes of *HSFA6a* were recovered, and the greening ratios were higher than those of wild type (Figure 6C and D). In a parallel experiment, we treated *HSFA6a-OE/*C and *HSFA6a-OE/*p transgenic plants with drought and investigated the survival rates after re-watering. The results showed that *HSFA6a-OE/*C plants were more tolerant to drought and had higher survival rates than wild type (Figure 6E and F), consistent with the previous report (Hwang et al., 2014). However, the *HSFA6a-OE/*p transgenic plants were more sensitive to drought and had lower survival rates than wild type (Figure 6E and F), indicating that mutation of *AtPTPN* changed the role of *HSFA6a* in plant drought tolerance. Taken together, these results implied that the function of *HSFA6a* in ABA and drought responses might depend on *AtPTPN* activity.

DISCUSSION

In this study, we characterized the function of *PTPN* in plant drought tolerance. We showed that loss of function mutants, including *Atptpn-1* T-DNA insertion and *Atptpn-2* mutants, were hyposensitive to ABA treatments and hypersensitive to drought. The expression of *AtPTPN* was detected in multiple tissues and up-regulated by both ABA and drought stresses. We showed that the *PTPN* gene encodes an enzyme with nucleotidase activity. Since it released Pi via hydrolyzing the nucleotides GDP/GMP/dGMP/IMP/dIMP, it helped regulate AsA biosynthesis. We further demonstrated that the TF HSFA6a, whose expression is directly activated by ABF TFs in an ABA-dependent manner in drought response (Hwang et al., 2014, Supplemental Figure S12), directly bound to the HSE of the *AtPTPN* promoter, and *HSFA6a* and *AtPTPN* functioned synergistically to regulate plant drought tolerance. These data together provided evidences for a working model in which drought activated the expression of *AtPTPN* via ABF-HSFA6a pathway. AtPTPN then functioned to increase the endogenous Pi contents of cells to enhance AsA production and subsequently positively regulate plant drought tolerance (Figure 7).

Journal Pre-proof

AtPTPN is a novel nucleotidase specifically targeting limited purine nucleotides.

Previous studies have revealed that FERY/SAL1 has at least two enzymatic activities in plants. It acts as a 3'(2'), 5'-bisphosphate nucleotidase and inositol polyphosphate 1-phosphatase (Quintero et al., 1996). There are various putative substrates of SAL1, including phosphoadenosine phosphosulphate (PAP), adenosine 3',5'-bisphosphate (PAP) and inositol polyphosphates (IPs) (Quintero et al., 1996; Xiong et al., 2004; Wilson et al., 2009; Rodríguez et al., 2010). An enzymatic motif of HCxxGxxR(T/S) is important in hydrolyzing inositol polyphosphates, such as inositol hexaphosphate, or phytate (IP6) (Chu et al., 2004). Two similar motifs (NCxxGxxRT) were found in all PTPNs collected from various organisms in this study (Supplemental Figure S3). We thus speculated PTPN may have a phytase activity. Surprisingly, neither AtPTPN nor ZmPTPN had enzymatic activity towards IP6 (Supplemental Figure S10A). The HCxxGxxR(T/S) motif forms a P loop for binding to phytate, and the amino acid His (H) in this motif is important for P loop formation (Chu et al., 2004). There is one amino acid difference between the motifs in PTPN and that in phytase (N/H). The different amino acid may result in a conformational difference, resulting in different substrate preferences.

A number of chemicals were used for PTPN substrate screening in this study. Several nucleoside monophosphates or diphosphates, including IMP/dIMP, GMP/dGMP and GDP were hydrolyzed by both AtPTPN and ZmPTPN, showing that plant PTPNs have nucleotidase activities (Figure 3, Supplemental Figure S10). The inosine monophosphate (IMP) is a precursor in the biosynthesis of purine monophosphates, such as adenosine monophosphate (AMP) and guanosine monophosphate (GMP), in both animals and plants. Xanthylate (XMP) is an intermediate in the reaction converting IMP into GMP, and thus has a molecular structure like IMP (Barsotti et al., 2005). PTPN hydrolyzed IMP and GMP, but not AMP nor XMP or other chemicals analyzed, indicating the substrate specificities of plant PTPNs. Thus far, there is very limited functional validation of plant nucleotidases. Our findings indicated that PTPN could be a novel nucleotidase in plant because it

specifically targets very limited purine nucleotides, which is different from SAL1, and has important roles in plant stress tolerance. The molecular insights of how PTPN hydrolyze the substrates are currently unknown. In future, it is worth of dissecting the functional amino acids or motifs of PTPN via protein crystal-structure analysis.

PTPN might be an important regulator of oxidative stress responses

GDP-D-mannose-3,5-epimerase (GME) is an important AsA synthetic enzyme converting GDP-D-mannose into GDP-L-galactose (Wheeler et al., 1998). Overexpression of *MsGME* in Arabidopsis increases the AsA levels in the transgenic plants and enhances the drought tolerance of these plants (Ma et al., 2014). Exogenous application of AsA enhances the drought tolerance of various plant species, including maize (Darvishan et al., 2013), wheat (Malik and Ashraf, 2012; Hussein et al., 2014), sunflower (Ahmed et al., 2013), savory (Yazdanpanah et al., 2011), okra and canola (Amin et al., 2009; Shafiq et al., 2014). Our study also showed that overexpression of VTC2, the rate-limiting enzymes in AsA biosynthesis, greatly enhanced the plant drought tolerance (Figure 4). Our data have demonstrated positive roles of PTPN in control of AsA production via releasing of endogenous Pi in plant drought responses. *Atptpn-1* mutants still had some AsA levels indicated that the plants can use Pi from multiple sources to make their AsA.

During drought or other abiotic stresses, and even in biotic stresses, production of many ROS molecules, including H_2O_2, singlet oxygen and superoxide anion radicals is enhanced. These over-accumulated ROS cause oxidative stress to the membrane lipids or DNA, RNA and protein molecules (Mittler, 2017). AsA is the maximum water-soluble antioxidant compound present in plant tissues that can directly scavenges ROS molecules and protects the membrane systems from oxidative stress (Gallie, 2013; Akram et al., 2017). There were lower AsA levels in the *Atptpn-1* mutants as compared to wild type plants. The H_2O_2 contents and MDA levels in *Atptpn-1* mutants were significantly higher than those in wild type plants (Figure 1). Thus, *Atptpn-1* mutants partially lost their abilities in scavenging ROS molecules and reducing oxidative stress, and that might result in the sensitivity of *Atptpn-1* mutants to drought.

Journal Pre-proof

To our knowledge, PTPN is the only nucleotidase identified so far to regulate AsA production. Given that AsA is the main anti-oxidant in plant, our data suggest that PTPN might play important roles in multiple stress responses via anti-oxidative mechanisms.

AtPTPN acts in the nexus of ABA signaling and AsA biosynthesis pathways

It has been reported that the HSF transcription factors generally bind to the canonical *cis*-element nGAAnnTTCn (von Koskull-Döring et al., 2007). A recent study demonstrated that HSFA1a positively regulated drought tolerance by binding the canonical HSE of autophage genes (ATGs) and regulating their expression (Wang et al., 2015). Besides the canonical HSE, a previous study based on chromatin immunoprecipitation (ChIP) has revealed six putative novel HSFA1a binding-motifs that can be classified into three groups: gap-type, TTC-rich-type and stress responsive element (STRE) (Guo et al., 2008). There is a TTC-rich-type HSE motif (TTTCCGGGATTCG) in the *AtPTPN* promoter (Figure 4). The EMSA and Chip-qPCR results demonstrated that HSFA6a could directly bind to this HSE motif in the *AtPTPN* promoter. Thus, the subfamily A HSF TFs could regulate the expression of downstream genes by binding various HSE motifs in response to drought.

There was reduced ABA levels in *Atptpn-1* and *Atptpn-2* mutants and the ABA signaling was impaired in these mutants (Figure 1), suggesting that *AtPTPN* might regulate drought tolerance in an ABA-dependent manner. Arabidopsis *HSFA6a* has been previously reported to play roles in plant drought responses. Our experiments indicated that drought-activated *HSFA6a* is dependent on ABA signaling (Supplemental Figure S12). Plants overexpressing *HSFA6a* have increased ABA sensitivity and drought tolerance (Figure 5; Hwang et al., 2014). ABF transcription factors are known to be phosphorylated and activated by ABA signaling, and positively regulate plant drought tolerance (Yoshida et al., 2010; Fujita et al., 2013). The expression of *HSFA6a* has been activated by ABA via binding of ABFs to the ABA responsive elements (ABRE) in the *HSFA6a* promoter (Hwang et al., 2014). The enhanced expression of *AtPTPN* in *HSFA6a-OE*/C plants indicated that HSFA6a activated the expression of *AtPTPN*.

Binding of HSFA6a to the HSE motif of the *AtPTPN* promoter indicated that *AtPTPN* could be a direct target of HSFA6a in drought responses. Additionally, the function of HSFA6a in response to ABA and drought largely depended on AtPTPN activities (Figure 5). Therefore, AtPTPN likely functions in the nexus of ABA signaling and AsA biosynthesis pathways to control plant drought tolerance (Figure 7). Given the conservation of *PTPN* in plant drought tolerance (Supplemental Figure S7 and S8), this gene may have a potential use in genetic engineering for breeding of drought-tolerant crops.

Journal Pre-proof

METHODS

Plant Materials and Growth Conditions

Arabidopsis thaliana ecotype Col-0 was used as the wild type in this study. The T-DNA insertion mutants of *Atptpn-1* (SALK_023939) were ordered from the ABRC. The T-DNA insertion mutants were verified by genotyping and expression assays with primers SALK_LB1.3, *Atptpn-1*-F/R and Actin3-F/R. The *ost1*, *snrk2.2*/*3*/*6*, *abf3*/*4* mutants were reported previously (Fujii and Zhu, 2009; Fujita et al., 2013). Seeds were first vernalized for 3d at 4℃ in the dark after su rface-sterilized with 10% bleach and 0.025% Triton x-100 for 10 min, washed with sterile distilled water three times, and then germinated on full-strength MS plates (4.4 g/L MS powder, 10 g/L sucrose, and 8 g/L agar, pH 5.7) and grown in a growth chamber at 22℃ (light period: 16 h light/8 h dark, illumination: 5800 Lux, relative humidity: 60±5%). Ten-day-old seedlings were transferred into soil and grown in a culture room (light period: 16 h light/8 h dark, illumination: 8000 Lux, relative humidity: 70±5%, temperature: 22-24℃).

Bioinformatics Analysis

To explore the phylogenesis of *PTPN* genes, blast against multiple plant species genome in EnemblPlants(http://plants.ensembl.org/ index.html) was performed. The Arabdopsis PTPN sequence was used as query in this assay. Full-length amino acid sequences of all identified PTPN genes were aligned using MUSCLE built-in MEGA6(https://www.megasoftware.net/) with default parameters. Then phylogenic tree was constructed by MEGA6 using neighbor joining (NJ) method with following parameters: pairwise deletion, uniform rates and bootstrap (1000 times). Meanwhile, all aligned PTPN sequences were submitted to Weblogo (http://weblogo. berkeley.edu/logo.cgi) to make seqlogo figure.

Plant Transformation

CRISPR/Cas9-based genome editing technology was used in this study to generate *Atptpn-2* gene editing *Arabidopsis* lines. The effective guide RNA of *AtPTPN* was predicted and obtained from web-based *CRISPR PLANT* software (http://www.genome.arizona.edu/crispr/CRISPRsearch.html) (gRNA1:

GATACCGAAGGAGCCAGAGC, gRNA2: CAGATCGAAGGCGCTCCTAA). Two gRNAs of *AtPTPN* were cloned into gRNA backborn by PCR using pCBC-DT1T2 as temples with primers gRNA1-F/R and gRNA2-F/R, and then the *AtPTPN* gRNA backbone were inserted into pHEE401 vector by T4 ligase, BsaI was used in the linearization of pHEE401 to produce pHEE401-*AtPTPNCrispr*. The recombinant plasmids were transformed into *Agrobacterium tumefaciens* stain GV3101. Agrobacterium-mediated transformation into the wild type (Col-0) was performed by the floral dip method. Positive transformants were selected on MS plates containing 25 μg/ml hygromycin. Homozygous lines were identified by amplifying fragments surrounding the target sites of *AtPTPN* with gene-specific primers Crispr-CX-F/R and confirmed by sequencing.

For overexpression of *AtPTPN*, the coding sequence (CDS) of *AtPTPN* was amplified by PCR using Arabidopsis cDNA as template with primers AtPTPN-F'/R', and then inserted into pCAMBIA1305-3HA by using the recombination kit (Vazyme). Kpn I and Xba I were used in the linearization of pCAMBIA1305-3HA to generate pCAMBIA1305-*AtPTPN-3HA*. The recombinant plasmids were transformed into *Agrobacterium tumefaciensstain* GV3101. Agrobacterium-mediated transformation of wild type (Col-0) and *Atptpn-1* mutants was performed by the floral dip method. Positive transformants were selected on MS plates containing 25 μg/ml hygromycin. Single copy lines were decided based on a ratio of 3:1 (survival/dead) on selective MS plates. Homozygous lines were used for further analysis.

For GUS staining assay, 2000bp DNA fragment before translation start sites of *AtPTPN* was cloned with primers *AtPTPNpro*-F/R and inserted into pCAMBIA1300-*GUS* vector to promote the expression of *GUS* genes. The pCAMBIA1300-*AtPTPNpro*-GUS plasmids were introduced into Agrobacterium tumefaciens strain GV3101 and transformed into Arabidopsis Col-0 ecotype using the flower dip method. Positive transformants were selected on MS plates containing 50 μg/ml basta. The homozygous lines showed stable expression of *GUS* were selected for further analysis.

For overexpression of *VTC2*, the coding sequence (CDS) of *VTC2* was amplified by PCR using Arabidopsis cDNA as temples with primers VTC2'-F/R, and then inserted

Journal Pre-proof

into pCAMBIA1305-3HA, Kpn I and Sal I were used in the linearization of pCAMBIA1305-*3HA* to generate pCAMBIA1305-*VTC2-3HA*. For overexpression of *AtHSFA6a*, *AtHSFA6a* was amplified by PCR using Arabidopsis genome DNA as temples with primers AtHSFA6a-F/R and then inserted into pCAMBIA1305-3HA, Kpn I and Xba I were used in the linearization of pCAMBIA1305-*3HA* to generate pCAMBIA1305-*AtHSFA6a-3HA*. The recombinant plasmids were transformed into Agrobacterium tumefaciensstain GV3101. Agrobacterium-mediated transformation into the wild type (Col-0) and *Atptpn-1* mutants was performed by the floral dip method. Positive transformants were selected on MS plates containing the 25mg/ml hygromycin. Single copy lines were decided based on a ratio of 3:1 (survival/dead) on selective MS plates. Homozygous lines were used for further analysis.

For overexpression of *ZmPTPN* in maize, *ZmPTPN* CDS was amplified by RT-PCR using cDNA of B73 as template with primers ZmPTPN-F/R. The fragment was inserted into pZZ0153 by recombination kit (Vazyme). Xma I and Asc I were used in the linearization of pZZ0153 to produce pZZ0153-ZmPTPN vector. For RNA interference (RNAi) of *AtPTPN*, PDKin (PDK intron) fragments were amplified by PCR using pSAT6-PDKin as templates with PDKin-F/R as primers, and then inserted into pZZ0153. Sma I was used in the linearization of pZZ0153 to produce pZZ0153-PDKin vector. *ZmPTPN* (RNAi) fragments were amplified by PCR using DNA of B73 as templates with *ZMPTPN* (RNAi)-F/R as primers, and then inserted into the flanking sides of the PDKin fragment in pZZ0153-PDKin by T4 ligase, Spe I and Pme I were used in the linearization of pZZ0153-PDKin to produce pZZ0153- *ZMPTPN* (RNAi)-PDKin vector. XmaI and AscI were used in the linearization of pZZ0153- *ZMPTPN*(RNAi)-PDKin to produce pZZ0153- *ZMPTPN* (RNAi)-PDKin-*ZMPTPN*(RNAi) vector (the insertion directions of the two ZmPTPN (RNAi) fragments are opposite). China National Seed Group Co., Ltd did the gene transformation using C01 inbred as the receptor.

Abiotic Stress Treatments

For the ABA treatments, seeds were sown on MS medium plates with different concentrations of ABA (Sigma-Aldrich) for 5-6 days and then cotyledon greening was

determined under a microscope. To observe the phenotype of root length, seeds were germinated and grown vertically on MS plates for 4 days and then transferred onto fresh MS plates with different concentrations of ABA for 10 days, and then the root length was calculated using Image J software. For the osmosis stress tolerance test, seeds were germinated and grown vertically on MS for 4 days, then transferred onto MS plates with different concentrations of mannitol for 10 days, and then the root length, fresh weight of shoot and contents of proline and anthocyanin were detected.

For qRT-PCR expression assays, seeds were germinated and grown vertically on MS plates for 2-weeks, and then treated with 100 μM ABA in liquid full-strength MS medium or dehydrated on dry filter paper for various periods and then frozen in liquid nitrogen for further analyses. For the drought stress experiments, plants were grown for 3 weeks in a growth chamber with light period: 16 h light/8 h dark, illumination: 8000 Lux, relative humidity: 70±5%, temperature: 22-24℃ , soil moisture (garden soil): ~90% and subjected to drought stress by withholding watering for 14±2 days (the exact days for each treatment were shown in the Figures/legends). The plants were rewatered and survived plants were counted three days after rewatering. For maize drought experiments, imbibed seeds were grown in soil in greenhouse (approximately 30℃) under normal watering condition (field soil with moisture: 30~40%) until 4-leaf stage, and the plants were subjected to drought stress for 10 days. The plants were rewatered and the survived plants were counted 7 days after rewatering. In the parallel experiments, leaves from plants were harvested after drought treatment for 10 days, and the ascorbic acid, proline, hydrogen peroxide (H_2O_2) and malondialdehyde (MDA) contents were determined. For all the above assays, at least three independent experiments were performed.

Pi treatment

For pi treatment, Col-0 and *Atptpn-1* seeds were germinated and grown on MS plates for 7 days and then transferred into soil and grown at 22-24℃ under long-day conditions (16 h light/8 h dark). Four weeks later after the transplanting, the plants were watered with 1 mM KH2PO4 (+Pi) or 1 mM KCl (CK, -Pi) every two days. Five days

later after the treatments, the rosette leaves of the plants were harvested for AsA content measurement.

Histochemical GUS Staining

The histochemical GUS Staining were performed as described in our previous report (Dai et al.,2012) with minor modifications. Briefly, tissues from different developmental stages of *AtPTPNpro*:*GUS* transgenic plants were collected and submerged in GUS staining solution [50 mM sodium phosphate, pH 7.0, 0.5% Triton X-100, 5 mM EDTA, 0.5 mM $K_3Fe(CN)_6$, 0.5 mM $K_4Fe(CN)_6$, and 2 mM 5-bromo-4-chloro- 3-indolyl glucuronide] at 37℃ for 16h. To remove chlorophyll after GUS staining, the tissues were immersed in acidic acid/alcohol (6:1) and mounted with the mixture of chloral hydrate/distilled water/glycerol (8:3:0.5) before observation with a light microscope. The digital images were taken with the Nikon NIS Elements D software.

RNA Purification and Expression Analysis

Total RNA was isolated from the seedlings with Trizol reagent according to the manufacturer's instructions (Thermo). 1.5 μg of total RNA was used for reverse transcription with M-MLV reverse transcriptase and oligo (dT) primers according to the manufacturer's instructions (Promega). Single-stranded cDNA was used for expression analyses. At least three biological replicates per experiment were sampled, and each sample was run in triplicate. The Arabidopsis *actin* gene was used as an internal control to normalize the data. For each primer pair, the amplification efficiency was checked by a melting-curve analysis.

Protein Isolation and Enzymatic Assays

Protein expression and purification were performed as previously described (Wang et al., 2016). Briefly, *AtPTPN* and *ZmPTPN* were amplified by PCR using cDNA of Col-0 or B73 as templates with primers *AtPTPN*-S-F/R and ZmPTPN-C-F/R respectively, and then *AtPTPN* fragments were inserted into modified pFastBac1 vector with a SUMO affinity tag fused to the N terminus. *ZmPTPN* fragments were inserted into modified pFastBac1 vector with a His affinity tag fused to the C terminus by using the recombination kit (Vazyme). BamH I/Xho I and Nde I/Xho I were used in the

linearization of pFastBac1-Sumo and pFastBac1-His to produce pFastBac1-Sumo-AtPTPN and pFastBac1-ZmPTPN-His vector, respectively. Bacmids were generated in DH10Bac cells following the instructions for the Bac-to-Bacbaculovirus expression system (Invitrogen) and baculoviruses were generated and amplified in Sf-9 insect cells. For protein expression and purification, Cells were harvested by centrifugation at 2,000g for 15 min and homogenized in ice-cold lysis buffer containing 25 mM Tris-HCl, pH 8.0, 150 mM NaCl and 0.5 mM phenylmethanesulfonyl-fluoride (PMSF). The cells were disrupted using a cell homogenizer. The insoluble fraction was precipitated by ultracentrifugation (20,000g) for 1 h at 4℃. The supernatant was loaded onto a Ni-NTA superflow affinity column (Qiagen) and washed three times with lysis buffer plus 10 mM imidazole. Elution was performed in buffer containing 25 mM Tris-HCl, pH 8.0, and 250 mM imidazole. The purified protein was used for enzyme activity assays.

Enzymatic assays were performed as previously described (Kuznetsova et al., 2005) with minor modification. Briefly, for substrate screening assay, the reactions were performed in 96-well microplates using 160 µl reaction mixtures containing 50 mM HEPES–KOH (pH 7.5), 0.25 mM substrate and 1 µg of enzyme protein at 37℃ for 20 min. Activity profiles of AtPTPN and ZmPTPN were determined at different temperature, pH and divalent metal ion. The optimum temperatures of AtPTPN and ZmPTPN were determined by incubating the assay mixture at different temperatures in the range of 20 to 70℃ for 15 min in HEPE-KOH buffer pH7.5 with 1 µg protein and 0.25 mM substrate. The optimum pH of AtPTPN and ZmPTPN were determined by incubating the assay mixture at different buffer with different pH in the range of 2.5 to 8.0 for 15 min with 1 µg protein and 0.25 mM substrate. The following buffers were used for the indicated pH range: glycine-HCl, pH 2.5-4; Na acetate-acetic acid, pH 4.5-5.5; Tris-acetic acid, pH 6.0-6.5; HEPE-KOH, pH7.0-8.0; The optimum divalent metal ion for AtPTPN and ZmPTPN were determined by adding 0-10 mM divalent metal ion (Ca^{2+}, Mg^{2+}, Mn^{2+}, Cu^{2+}) into the reaction mixtures (50 mM HEPE-KON buffer PH7.5 with 1µg protein and 0.25 mM substrate) and incubating the reaction at 30 ℃ for 15min. All reactions were terminated by addition of 40 µl of Malachite Green reagent and the production of Pi was

measured at 630 nm 5 min later. All reactions were done in triplicate. Results were compared to a standard curve prepared with inorganic phosphate (KH_2PO_4). The enzyme activity was defined as the activity that released phosphate per min per mg enzyme protein under specified assay conditions.

Water loss assay

For water loss measurements, the detached leaves from 3-week-old plants were exposed to air at room temperature (~25℃) and weig hed at 100 min intervals using a microbalance. Water loss rates were recorded at 500 min after dehydration and measured as a percentage of the initial weight of fully hydrated leaves.

Stomatal aperture assay

Stomatal aperture was measured essentially as previously described (Ding et al. 2015). Briefly, epidermal peels from rosette leaves of 3-week-old Arabidopsis plants were floated in the stomatal opening solution (10 mM KCl, 50 μM $CaCl_2$, 10 mM MES, pH 6.15) and exposed to light for 2-2.5 h to achieve full opening of stomata. Subsequently, ABA was added to the opening solution to the final concentration of 0 or 10 μM and incubated for 1 hour to induce stomatal closure. After incubation, stomatal apertures were photographed and measured (width/length) in the presence or absence of 10 μM ABA (at least 40 stomatal apertures were measured for each) using the Image J software.

Subcellular-Localization of AtPTPN

To express the GFP-AtPTPN fusion protein, the coding regions of *GFP* were amplified by PCR using pSAT6-TAG as templates with primers GFP-F/R, and then inserted into pRTL2, Sac I and Xba I were used in the linearization of pRTL2 to generate pRTL2-*GFP*. Next, the coding regions of *AtPTPN* were amplified with primers AtPTPN (C) -F/R and then inserted into the vectors pRTL2-*GFP* by using the recombination kit (Vazyme). BamH I and Xba I were used in the linearization of pRTL2-*GFP* to generate pRTL2-*GFP-AtPTPN*. The plasmids were used for protoplast transformation according to a protocol developed by Jen Sheen (http://genetics.mgh.harvard.edu/sheenweb/). After transformation, the protoplasts

were incubated at 22 ℃ in dark for 16 h. Then the fluorescence signals of GFP were examined with a confocal microscope (Leica).

Yeast one Hybrid Assay

The yeast one hybrid assay was performed using MATCHMAKER One-Hybrid System (PT1031-1). Briefly, DNA fragments from the promoter of *AtPTPN* (P1, P2, P3 and P4) were amplified from DNA of Col-0 with primers *PTPNpro*-F1/R1, *PTPNpro*-F2/R2, *PTPNpro*-F3/R3 *and PTPNpro*-F4/R4 respectively. And then *AtPTPN* promoter fragments were inserted into pHISi-1 plasmid as baits to trap a protein which can bind to the promoter of *AtPTPN*. The library of Arabidopsis transcription factors was used in this assay. The yeast strain YM4271 and Y187 was used for bait clones and prey clones. Strains containing the various transcription factors protein or fragments of *AtPTPN* promoter were mated pairwise and screened on His-Trp- dropout media, 3-AT was used to suppress background growth in this experiment.

Electrophoretic Mobility Shift Assay

The *HSFA6a* gene was cloned into the pGEX-4T containing a N-terminal GST-coding sequence. The fusion and empty constructs were respectively transformed into BL21 *E. coli* cells. The fusion proteins were purified according to the manufacturer's procedure. The probes were created by annealing together complementing biotinylated oligonucleotides. Electrophoretic mobility shift assays (EMSA) were performed using a LightShiftChemiluminescent EMSA kit (Thermo Scientific). Each binding reaction contains 40 fmol of biotin-labeled probe, 5 μg protein. The unlabeled probes were used as competitors. A 5% polyacrylamide gel in 0.5X TBE pre-run for 40 minutes at 4℃. Five μl of 5X loading buffer were added to each binding reaction, and subsequently each reaction was subjected to gel electrophoresis at 100 V for 1 h. The probes and proteins on the gel were then transferred to a charged nylon membrane (100 V, 50 min), and subsequently the membrane was UV cross-linked at 120 mJ/cm^2 for 1 min. The membrane was treated with developing buffers according to the manufacturer's protocol and then exposed to film and developed.

Luciferase Assay

The P4 fragment derived from At*PTPN* promoter was cloned into pGL3-Basic to drive the expression of firefly luciferase reporter. The effecter *HSFA6a* was cloned into pRTL2 after the 35S promoter. Arabidopsis leaf protoplasts were isolated from 4-week-old soil-grown plants and inoculated with various constructs according to a protocol developed by Jen Sheen lab (http://genetics.mgh.harvard.edu/sheenweb/). After transformation, the protoplasts were incubated at 22℃ for 16h. Firefly and Renilla luciferase were quantified with a dual-luciferase reporter assay according to the manufacturer's instructions (Promega). Three independent transformation assays were used to calculate the mean and SE for luciferase expression.

ChIP Assay

ChIP assays were performed as previously described (Kaufmann et al., 2010). Briefly, 3-week-old Col-0 and *HSFA6a*-OE/Col-0 seedlings (about 2 g) were cross-linked in 1% formaldehyde for 25 min. Then the nuclei were isolated and resuspended in high salt nuclear lysis buffer. Chromatin was sonicated to an average size of 100-500 bp using the Bioruptor (Diagenode). The protein-DNA complex was immunoprecipitated by a mouse HA antibody (NewEast, Cat. # 28003). After elution, reverse crosslinking, the enriched DNA was purified for qPCR.

Measurement of Anthocyanin

The experiments were performed as described by previous report (Mancinelli, 1990) with minor modifications. Briefly, 20 mg rosette leaves from seedlings were collected and placed in 2 mL of extraction solution (1% HCl in methanol) at 4 ℃ for 16 h. The absorbance of extracts was measured at A530 and A657. The quantity of anthocyanin was determined as A530 − 0.25 × A657.

Measurement of melondialdehyde (MDA)

Extraction was performed by homogenisation of 0.2 g leaf tissue with 2 ml 5 % (w/v) trichloroacetic acid and centrifugation at 12000 rpm for 10 min. Then 1.5 ml 5 % trichloroacetic acid-containing 0.67 % (w/v) thiobarbituric acid was added to 1.5 ml of the supernatant. The mixture was boiled for 30 min, quickly cooled on ice and centrifuged at 12000g for 5 min. The absorbance of extracts was measured at A450,

A532 and A600. The quantity of melondialdehyde was determined as C (μM/L) =6.45 (A532-A600)-0.56A450.

Measurement of Hydrogen Peroxide

Quantitative assay of H_2O_2 was performed essentially as described previously (Li et al., 2019) by using the Amplex® Red Hydrogen Peroxide assay kit (Cat. No. A22188, Invitrogen). Briefly, about 100 mg leaves were harvested and immediately frozen in liquid nitrogen. The frozen leaves were ground to fine powder and extracted with 1 ml of 1 × reaction buffer (50 mM sodium phosphate, at pH 7.4), and 10 μl of the dissolved sample was diluted with 490 μl of 1× reaction buffer, of which 100 μl was used for the assay. Reaction mixtures (100 μl of the sample and 100 μl of Amplex Red reagent/HRP working solution) were incubated in 96-well plates for 30 min at room temperature in dark. A microplate reader (SpectraMax® i3X) was employed to detect the absorbance of H_2O_2 at 560 nm. The H_2O_2concentration was calculated using a standard curve according to the manufacturer's protocol.

Measurement of Proline

Two hundred mg leaves were homogenized in 5 ml 3% sulfosalicylic acid. The mixture was boiled for 10 min and then centrifuged at 3000g for 20 min. Then 1 ml sample supernatant was mixed with 1 ml acetic acid and 1 ml ninhydrin reagent in 10ml tube and boiled for 30 min, then cooled on ice. Equal volume of toluene was added to each sample and vibrated for 1 min, and then centrifuge at 1000g for 5 min. The absorbance of supernatant was measured at A520 by spectrophotometer and then the contents of proline were calculated using the standard curve.

Measurement of Ascorbate Acid

Measurement of ascorbate acid was performed as previously described (Miyaji et al., 2015). About 100 mg of leaves were harvested and immediately frozen in liquid nitrogen. The frozen leaves were ground to a fine powder and extracted with 1 ml of 0.2 N HCl for 30 min at 4 ℃ and then centrifuged at 16,000g for 10m in at 4 ℃. The 0.5 ml supernatant and AsA standards were neutralized with NaH_2PO_4 (pH 5.6) and NaOH as follow: first, 50 ul of 0.2 M NaH_2PO_4 (pH 5.6) was added, followed by added 0.5ml of

0.2 M NaOH. and the pH was verified with pH indicator paper. The final pH of all samples was between 5 and 6. And then the neutralized supernatant was pretreated with 5mM DTT for 30 min at room temperature. Next, 100 ul supernatant or AsA standards (0, 0.25, 0.5, 0.75, 1.5 mM) was add to 250 ul of 0.2 M NaH_2PO_4 (pH 5.6) and 148 ul double distilled water. Total ascorbate was determined by the change in absorbance at 265 nm after the addition of 2 ul (0.5 units) of ascorbate oxidase (sigma-A0157) to the mixture. The contents of total ascorbate were calculated using the standard curve.

Measurement of soluble Pi

The measurement of plant soluble Pi was performed as previously described with minor modifications (Gu et al., 2017). Briefly, ~0.2g fresh samples were homogenized in 1ml 10% (w/v) perchloric acid by using an ice-cold mortar and pestle. The homogenate was then diluted 10-fold with 5% (w/v) perchloric acid and placed on ice for 30 min. After centrifugation at 12000g for 10 min at 4℃, the supernatant was used for Pi measurement by using the molybdenum blue method: 4% (w/v) ammonium molybdate dissolved in 0.5 M H_2SO_4 (solution A) was mixed with 10% ascorbic acid (solution B) at a ratio of A:B=6:1. A 2ml aliquot of this working solution was added to 1 ml of the sample solution and incubated in a water bath at 42 ℃ for 20 min. After being cooled, the absorbance at 820 nm was measured by a spectrophotometer and then the contents of soluble Pi were calculated using the standard curve.

Measurement of ABA content

Up to 100 mg leaves were harvested, equally divided into two samples (sample #1, #2) and the fresh weights were determined (FW1 and FW2). Next, sample #1 (~50 mg) was dried at 65℃ for 24 hours and the dry mass were determined (DW1). Sample #2 was stored in liquid nitrogen immediately for ABA content measurement. Frozen leaf sample #2 (~50 mg) were ground to a fine power in liquid nitrogen using a pestle in 2-ml tube, and then mixed with 750 µl cold extraction buffer 1 (methanol:water:acetic acid, 80:19:1, v/v/v, supplemented with 10 ng ^{2H6}ABA as internal standards), vigorously shaken on a shaking bed for 16 h at 4℃ in dark, and then centr ifuged at 12,000 rpm for 15 min at

4℃. The supernatant was carefully transferred to a new 2-ml tube and the pellet was remixed with 400 µl extraction buffer 2 (methanol:water:acetic acid, 80:19:1, v/v/v) shaken for 4 h at 4℃, then centrifuged. The two su pernatants were combined and filtered using a syringe-facilitated 13-mm diameter nylon filter with pore size 0.22 µm. The filtrate was dried by evaporation under the flow of nitrogen gas for approximately 1 h at room temperature, and then resuspended in 200 µL methanol. ABA was quantified using LC-ESI-MS-MS system as previously described (Liu et al., 2012). The ABA concentration of samples (C: ng/ml) was calculated using the standard curve of ABA (sigma) ranging from 0 to 20 ng/ml. The ABA contents of samples were determined as: C∗0.2/ (DW1/FW1) ∗FW2.

Primers

All primers used in this study are listed in Supplementary Table 2.

SUPPLEMENTAL INFORMATION

Supplemental Information is available at *Molecular Plant Online*.

FUNDING

This work was supported by National Key Research and Development Program of China (2016YFD0100600), National Natural Science Foundation of China (31971954), the Thousand Talents Plan of China and the Fundamental Research Funds for the Central Universities of China (2662015PY170), partly supported by the open funds of the National Key Laboratory of Crop Genetic Improvement.

AUTHOR CONTRIBUTIONS

M.D. conceived the project. H.Z., Y.X., N.H., H.L. and L.F. performed the experiments. X.S., and F.Z. carried out the bioinformatics analysis. D.Z purified the proteins that were expressed in insect cells. X.L. managed the field growth of transgenic maize. M.D., H.Z., Y.X., and X.L. designed the experiments and analyzed the data. M.D. and H.Z. wrote the manuscript. W.T. and J.Y revised the article. All authors read and approved the final manuscript.

ACKNOWLEDGMENT

Journal Pre-proof

We thank Dr. Haiyang Wang (Biotechnology Research Institute, Chinese Academy of Agricultural Sciences) for discussion. No conflict of interest declared.

Journal Pre-proof

Journal Pre-proof

REFERENCES

Ahmed, F., Baloch, D.M., Hassan, M.J., and Ahmed, N. (2013). Role of plant growth regulators in improving oil quantity and quality of sunflower hybrids in drought stress. Biologia **59:**315-322.

Akram, N.A., Shafiq, F., and Ashraf, M. (2017). Ascorbic Acid-A Potential Oxidant Scavenger and Its Role in Plant Development and Abiotic Stress Tolerance. Front. Plant Sci. **8:**613.

Amin, B., Mahleghah, G., Mahmood, H.M.R., and Hossein, M. (2009). Evaluation of interaction effect of drought stress with ascorbate and salicylic acid on some of physiological and biochemical parameters in okra (Hibiscus esculentus L.). Res. J. Biol. Sci. **4:**380-387.

Badejo, A.A., Fujikawa, Y., and Esaka, M. (2009). Gene expression of ascorbic acid biosynthesis related enzymes of the Smirnoff-Wheeler pathway in acerola (Malpighia glabra). J. Plant Physiol. **166:**652-60.

Barsotti, C., Pesi, R., Giannecchini, M., and Ipata, P.L. (2005). Evidence for the involvement of cytosolic 5'-nucleotidase (cN-II) in the synthesis of guanine nucleotides from xanthosine. J. Biol. Chem. **280:**13465-9.

Bulley, S.M., Rassam, M., Hoser, D., Otto, W., Schünemann, N., Wright, M., MacRae, E., Gleave, A., and Laing, W. (2009). Gene expression studies in kiwifruit and gene over-expression in Arabidopsis indicates that GDP-L-galactose guanyltransferase is a major control point of vitamin C biosynthesis. J. Exp. Bot. **60:**765-78.

Choudhury, F.K., Rivero, R.M., Blumwald, E., and Mittler, R. (2017). Reactive oxygen species, abiotic stress and stress combination. Plant J. **90:**856-867.

Chu, H.M., Guo, R.T., Lin, T.W., Chou, C.C., Shr, H.L., Lai, H.L., Tang, T.Y., Cheng, K.J., Selinger, B.L., and Wang, A.H. (2004). Structures of Selenomonas ruminantium phytase in complex with persulfated phytate: DSP phytase fold and mechanism for sequential substrate hydrolysis. Structure **12:**2015-24.

Conklin, P.L., Gatzek, S., Wheeler, G.L., Dowdle, J., Raymond, M.J., Rolinski, S., Isupov, M., Littlechild, J.A., and Smirnoff, N. (2006). Arabidopsis thaliana VTC4

encodes L-galactose-1-P phosphatase, a plant ascorbic acid biosynthetic enzyme. J. Biol. Chem. **281:**15662-70.

Conklin, P.L., Norris, S.R., Wheeler, G.L., Williams, E.H., Smirnoff, N., and Last, R.L. (1999). Genetic evidence for the role of GDP-mannose in plant ascorbic acid (vitamin C) biosynthesis. Proc. Natl. Acad. Sci. USA **96:**4198-203.

Conklin, P.L., Saracco, S.A., Norris, S.R., and Last, R.L. (2000). Identification of ascorbic acid-deficient Arabidopsis thaliana mutants. Genetics **154:**847-56.

Dai, M., Zhang, C., Kania, U., Chen, F., Xue, Q., McCray, T., Li, G., Qin, G., Wakeley, M., Terzaghi, W., et al. (2012). A PP6-type phosphatase holoenzyme directly regulates PIN phosphorylation and auxin efflux in Arabidopsis. Plant Cell **24:**2497-514.

Darvishan, M., Moghadam, H.R.T., and Nasri, M. (2013). Effect of foliar application of ascorbic acid (vitamin c) on yield and yield components of corn (Zea mays L.) as influenced by withholding of irrigation at different growth stages. Res. Crops **14:**736-742.

Ding, S., Zhang, B., and Qin, F. (2015). Arabidopsis RZFP34/CHYR1, a Ubiquitin E3 Ligase, Regulates Stomatal Movement and Drought Tolerance via SnRK2.6-Mediated Phosphorylation. Plant Cell **27:**3228-44.

Dowdle, J., Ishikawa, T., Gatzek, S., Rolinski, S., and Smirnoff, N. (2007). Two genes in Arabidopsis thaliana encoding GDP-L-galactose phosphorylase are required for ascorbate biosynthesis and seedling viability. Plant J. **52:**673-89.

Fujii, H., and Zhu, J.K. (2009). Arabidopsis mutant deficient in 3 abscisic acid-activated protein kinases reveals critical roles in growth, reproduction, and stress. Proc. Natl. Acad. Sci. USA **106:**8380-5.

Fujita, Y., Yoshida, T., and Yamaguchi-Shinozaki, K. (2013). Pivotal role of the AREB/ABF-SnRK2 pathway in ABRE-mediated transcription in response to osmotic stress in plants. Physiol. Plant **147:**15-27.

Gallie, D.R. (2013). The role of L-ascorbic acid recycling in responding to environmental stress and in promoting plant growth. J. Exp. Bot. **64:**433-43.

Gillespie, K.M., and Ainsworth, E.A. (2007). Measurement of reduced, oxidized and total ascorbate content in plants. Nat. Protoc. **2:**871-4.

Gu, M., Zhang, J., Li, H., Meng, D., Li, R., Dai, X., and Wang, S. (2017) Maintenance of phosphate homeostasis and root development are coordinately regulated by MYB1, an R2R3-type MYB transcription factor in rice. J. Exp. Bot. **68:**3603–3615.

Guo, L., Chen, S., Liu, K., Liu, Y., Ni, L., Zhang, K., and Zhang, L. (2008). Isolation of heat shock factor HsfA1a-binding sites in vivo revealed variations of heat shock elements in Arabidopsis thaliana. Plant Cell Physiol. **49:**1306-15.

Hernández, J.A, Jiménez, A, Mullineaux, P., and Sevilla, F. (2000). Tolerance of pea (Pisum sativum L.) to long-term salt stress is associated with induction of antioxidant defences. Plant Cell Environ. **23:**853–862.

He, Z., Zhong, J., Sun, X., Wang, B., Terzaghic, W., and Dai, M. (2018). The maize ABA receptors ZmPYL8, 9 and 12 facilitate plant drought resistance. Front. Plant Sci. **9:**422.

Himmelbach, A., Yang, Y., and Grill, E. (2003). Relay and control of abscisic acid signaling. Curr. Opin. Plant Biol. **6:**470-9.

Li, Y., Cao, X.L., Zhu, Y., Yang, X.M., Zhang, K.N., Xiao, Z.Y., Wang, H., Zhao, J.H., Zhang, L.L., Li, G.B., et al. (2019). Osa-miR398b boosts H_2O_2 production and rice blast disease-resistance via multiple superoxide dismutases. New Phytol. **222**:1507-1522.

Liu, H., Li, X., Xiao, J., and Wang, S. (2012). A convenient method for simultaneous quantification of multiple phytohormones and metabolites: application in study of rice-bacterium interaction. Plant Methods **8**:2.

Hussein, N.M., Hussein, M.I., Gadel Hak, S.H., and Hammad, M.A. (2014). Effect of two plant extracts and four aromatic oils on tuta absoluta population and productivity of tomato cultivar gold stone. Nat. Sci. **12:**108-118.

Hwang, S.M., Kim, D.W., Woo, M.S., Jeong, H.S., Son, Y.S., Akhter, S., Choi, G.J., and Bahk, J.D. (2014). Functional characterization of Arabidopsis HsfA6a as a heat-shock transcription factor under high salinity and dehydration conditions. Plant Cell Environ. **37:**1202-22.

Ioannidi, E., Kalamaki, M.S., Engineer, C., Pateraki, I., Alexandrou, D., Mellidou, I., Giovannonni, J., and Kanellis, A.K. (2009). Expression profiling of ascorbic

Journal Pre-proof

acid-related genes during tomato fruit development and ripening and in response to stress conditions. J. Exp. Bot. **60:**663-78.

Kaufmann, K., Muiño, J.M., Østerås, M., Farinelli, L., Krajewski, P., and Angenent, G.C. (2010). Chromatin immunoprecipitation (ChIP) of plant transcription factors followed by sequencing (ChIP-SEQ) or hybridization to whole genome arrays (ChIP-CHIP). Nat. Protoc. **5:**457-72.

Kuznetsova, E., Proudfoot, M., Sanders, S.A., Reinking, J., Savchenko, A., Arrowsmith, C.H., Edwards, A.M., and Yakunin, A.F. (2005). Enzyme genomics: Application of general enzymatic screens to discover new enzymes. FEMS Microbiol. Rev. **29:**263-79.

Leung, J., and Giraudat, J. (1998). Abscisic acid signal transduction. Annu. Rev. Plant Physiol. Plant Mol. Biol. **49:**199–222.

Linster, C.L., Gomez, T.A., Christensen, K.C., Adler, L.N., Young, B.D., Brenner, C., and Clarke, S.G. (2007). Arabidopsis VTC2 encodes a GDP-L-galactose phosphorylase,the last unknown enzyme in the Smirnoff-Wheeler pathway to ascorbic acid in plants. J Biol Chem. **282:**18879-85.

Ma, L., Wang, Y., Liu, W., and Liu, Z. (2014). Overexpression of an alfalfa GDP-mannose 3, 5-epimerase gene enhances acid, drought and salt tolerance in transgenic Arabidopsis by increasing ascorbate accumulation. Biotechnol Lett. **36:**2331-41.

Ma, Y., Szostkiewicz, I., Korte, A., Moes, D., Yang, Y., Christmann, A., and Grill, E. (2009). Regulators of PP2C phosphatase activity function as abscisic acid sensors. Science **324:**1064-8.

Malik, S., and Ashraf, M. (2012). Exogenous application of ascorbic acid stimulates growth and photosynthesis of wheat (Triticum aestivum L.) under drought. Soil Environ. **31:**72-77.

Mancinelli, A.L. (1990). Interaction between Light Quality and Light Quantity in the Photoregulation of Anthocyanin Production. Plant Physiol. **92:**1191-5.

Mittler, R. (2017). ROS Are Good. Trends Plant Sci. **22:**11-19.

Miyaji, T., Kuromori, T., Takeuchi, Y., Yamaji, N., Yokosho, K., & Shimazawa, A.,

Journal Pre-proof

Sugimoto, E., Omote, H., Ma, J.F., Shinozaki, K. et al. (2015). AtPHT4 is a chloroplast-localized ascorbate transporter in Arabidopsis. Nature Commun. **6**:5928.

Nover, L., Bharti, K., Döring, P., Mishra, S.K., Ganguli, A., and Scharf, K.D. (2001). Arabidopsis and the heat stress transcription factor world**,** how many heat stress transcription factors do we need? Cell Stress Chaperones **6:**177-89.

Ohama, N., Sato, H., Shinozaki, K., and Yamaguchi-Shinozaki, K. (2017). Transcriptional Regulatory Network of Plant Heat Stress Response. Trends Plant Sci. **22:**53-65.

Ou, B., Yin, K.Q., Liu, S.N., Yang, Y., Gu, T., Wing Hui, J.M., Zhang, L., Miao, J., Kondou, Y., Matsui, M., et al. (2011). A high-throughput screening system for Arabidopsis transcription factors and its application to Med25-dependent transcriptional regulation. Mol. Plant **4:**546-55.

Park, S.Y., Szostkiewicz, I., Korte, A., Moes, D., Yang, Y., Christmann, A., and Grill, E. (2009). Abscisic acid inhibits type 2C protein phosphatases via the PYR/PYL family of START proteins. Science **324:**1068-71.

Pastori, G.M., and Foyer, C.H. (2002). Common components, networks, and pathways of cross-tolerance to stress. The central role of "redox" and abscisic acid-mediated controls. Plant Physiol. **129:**460–468.

Quintero, F.J, Garciadeblás, B., and Rodríguez-Navarro, A. (1996). The SAL1 gene of Arabidopsis, encoding an enzyme with 3'(2'),5'-bisphosphate nucleotidase and inositol polyphosphate 1-phosphatase activities, increases salt tolerance in yeast. Plant Cell **8:**529–537.

Raghavendra, A.S., Gonugunta, V.K., Christmann, A., and Grill, E. (2010). ABA perception and signalling. Trends Plant Sci. **15:**395-401.

Rodríguez, V.M., Chételat, A., Majcherczyk, P., and Farmer, E.E. (2010). Chloroplastic phosphoadenosine phosphosulfate metabolism regulates basal levels of the prohormone jasmonic acid in Arabidopsis leaves. Plant Physiol. **152:**1335-45.

Shafiq, S., Akram, N.A., Ashraf, M., and Arshad, A. (2014). Synergistic effects of drought and ascorbic acid on growth, mineral nutrients and oxidative defense system in

canola (Brassica napus L.) plants. Acta Physiol. Plant **36:**1539-1553.

Shalata, A., Mittova, V., Volokita, M., Guy, M., and Tal, M. (2001). Response of the cultivated tomato and its wild salt-tolerant relative Lycopersicon pennellii to salt-dependent oxidative stress: The root antioxidative system. Physiol. Plant. **112:**487-494.

Smirnoff, N., and Pallanca, J.E. (1996). Ascorbate metabolism in relation to oxidative stress. Biochem. Soc. Trans. **24:**472–478.

Urzica, E.I., Adler, L.N., Page, M.D., Linster, C.L., Arbing, M.A., Casero, D., Pellegrini, M., Merchant, S.S., and Clarke, S.G. (2012). Impact of oxidative stress on ascorbate biosynthesis in Chlamydomonas via regulation of the VTC2 gene encoding a GDP-L-galactose phosphorylase. J. Biol. Chem. **287:**14234-45.

Valpuesta, V., and Botella, M.A. (2004). Biosynthesis of L-ascorbic acid in plants, new pathways for an old antioxidant. Trends Plant Sci. **9:**573-7.

von Koskull-Döring, P., Scharf, K.D., and Nover, L. (2007). The diversity of plant heat stress transcription factors. Trends Plant Sci. **12:**452-7.

Wang, X., Feng, J., Xue, Y., Guan, Z., Zhang, D., Liu, Z., Gong, Z., Wang, Q., Huang, J., Tang, C., et al. (2016). Structural basis of N(6)-adenosine methylation by the METTL3-METTL14 complex. Nature **534:**575-8.

Wang, Y., Cai, S., Yin, L., Shi, K., Xia, X., Zhou, Y., Yu, J., and Zhou, J. (2015). Tomato HsfA1a plays a critical role in plant drought tolerance by activating ATG genes and inducing autophagy. Autophagy **11:**2033-2047.

Wheeler, G.L., Jones, M.A., and Smirnoff, N. (1998). The biosynthetic pathway of vitamin C in higher plants. Nature **393:**365-9.

Wilson, P.B., Estavillo, G.M., Field, K.J., Pornsiriwong, W., Carroll, A.J., Howell, K.A., Woo, N.S., Lake, J.A., Smith, S.M., Harvey Millar, A., et al. (2009). The nucleotidase/phosphatase SAL1 is a negative regulator of drought tolerance in Arabidopsis. Plant J. **58:**299-317.

Xiang, Y., Sun, X., Gao, S., Qin, F., and Dai, M. (2017). Deletion of an Endoplasmic Reticulum Stress Response Element in a ZmPP2C-A Gene Facilitates Drought Tolerance of Maize Seedlings. Mol. Plant **10:**456-469.

Journal Pre-proof

Xiong, L., Lee, H., Huang, R., and Zhu, J.K. (2004). A single amino acid substitution in the Arabidopsis FIERY1/HOS2 protein confers cold signaling specificity and lithium tolerance. Plant J. **40:**536-45.

Yazdanpanah, S., Baghizadeh, A., and Abbassi, F. (2011). The interaction between drought stress and salicylic and ascorbic acids on some biochemical characteristics of Satureja hortensis. Afric. J. Agric. Res. **6:**798-807.

Yoshiba, Y., Kiyosue, T., Nakashima, K., Yamaguchi-Shinozaki, K., and Shinozaki, K. (1997). Regulation of levels of proline as an osmolyte in plants under water stress. Plant Cell Physiol. **38:**1095-102.

Yoshida, T. Fujita, Y., Sayama, H., Kidokoro, S., Maruyama, K., Mizoi, J., Shinozaki, K., and Yamaguchi-Shinozaki, K. (2010). AREB1, AREB2, and ABF3 are master transcription factors that cooperatively regulate ABRE-dependent ABA signaling involved in drought stress tolerance and require ABA for full activation. Plant J. **61:**672-85.

Yoshimura, K., Nakane, T., Kume, S., Shiomi, Y., Maruta, T., Ishikawa, T., and Shigeoka, S. (2014). Transient expression analysis revealed the importance of VTC2 expression level in light/dark regulation of ascorbate biosynthesis in Arabidopsis. Biosci. Biotechnol. Biochem. **78:**60-6.

Yu, H., Zhang, Y., Xie, Y., Wang, Y., Duan, L., Zhang, M., and Li, Z. (2017). Ethephon improved drought tolerance in maize seedlings by modulating cuticular wax biosynthesis and membrane stability. J. Plant Physiol. **214:**123-133.

Zhang, Z., Zhang, Q., Wu, J., Zheng, X., Zheng, S., Sun, X., Qiu, Q., and Lu, T. (2013). Gene Knockout Study Reveals That Cytosolic Ascorbate Peroxidase 2 (OsAPX2) Plays a Critical Role in Growth and Reproduction in Rice under Drought, Salt and Cold Stresses. PLoS ONE **8:**e57472.

Zhao, Y. Chan, Z., Gao, J., Xing, L., Cao, M., Yu, C., Hu, Y., You, J., Shi, H., Zhu, Y, et al. (2016). ABA receptor PYL9 promotes drought resistance and leaf senescence. Proc. Natl. Acad. Sci. USA **113:**1949-54.

Journal Pre-proof

Journal Pre-proof

Figure legends

Figure 1. ABA Hyposensitivity and drought hypersensitivity of *Atptpn* Mutants.

(A) and **(B)** The cotyledon phenotypes **(A)** and the percentages of cotyledon greening **(B)** in wild-type, *Atptpn-1* and *Atptpn-2* mutants in response to various concentrations of ABA. Col-0, *Atptpn-1* and *Atptpn-2* seedlings were grown on MS plates with 0, 0.5, 0.75, 1.0 μM ABA for 5 d. Data represent means±SD (n>150) from three biological replicates in **(B)**.

(C) and **(D)** A comparison of ABA-induced stomatal closure **(C)** and its statistical data **(D)** between Col-0, *Atptpn-1* and *Atptpn-2* plants treated with 0, 5, 10, 20 μM ABA. Red lines in **(C)** indicate the widest parts of the stomata. Bar=3 μm in **(C)**. Values represent means±SD (n>20) from three biological replicates in **(D)**.

(E) and **(F)** Drought-tolerant phenotypes **(E)** and survival rates **(F)** of soil-grown *Atptpn-1* and *Atptpn-2* mutants. Three-week-old plants were dehydrated for 16 days and then rehydrated for 3 days before phenotyping. Values in **(F)** represent means±SD obtained from three replicates with 30 plants each replicate.

(G) Water loss of leaves detached from Col-0, *Atptpn-1* and *Atptpn-2* mutant plants. Mean and SD of water loss rates were obtained from three replicates.

(H) to **(J)** The contents of proline **(H),** MDA **(I),** and H_2O_2 **(J)** in Col-0, *Atptpn-1* and *Atptpn-2* mutant plants with or without drought stresses. Values represent means±SD (n=3) from three biological replicates.

(K) and **(L)** ABA contents **(K)** and the expression of ABA responsive genes **(L)** in Col-0, *Atptpn-1* and *Atptpn-2* mutant plants with or without drought stress **(K)** or 100 μM ABA treatment **(L)**.

Statistical significance was determined by student *t*-test: $*P < 0.05$ and $**P < 0.01$.

Figure 2. The Expression Patterns of *AtPTPN* and subcellular localization of AtPTPN.

(A) Histochemical analysis of *AtPTPN::GUS* activity in different tissues. Panels show the GUS activities in roots**,** shoots**,** leaves, guard cells, flower and anthers. All GUS

staining patterns were obtained by observing at least 10 independent transgenic plants and typical pictures are shown. RC, root cap; VC, vascular cylinder; VT, vascular tissue; Vei, Vein; GC, guard cells; Pis, Pistil; Fil, Filament; Ovu, Ovule; Pol, Pollen.

(B) and **(C)** Time-course expression of *AtPTPN* in shoots **(B)** and roots **(C)** treated with or without 100 μM ABA. Values represent means ± SD (n=3) from three replicates.

(D) and **(E)** Time-course expression of *AtPTPN* in shoots **(D)** and roots **(E)** stressed with or without drought. CK, normal growth condition (without drought). Values represent means ± SD (n=3) from three replicates.

(F) Subcellular Localization of GFP-AtPTPN in leaf mesophyll protoplasts. Bars=20 μM

(G) Western blot assays showing the GFP and GFP-AtPTPN protein abundance in leaf mesophyll protoplasts.

(H) Subcellular Localization of GFP-AtPTPN and HY5-RFP (a nucleus marker) in leaf mesophyll protoplasts.

Statistical significance in panels **(B)** to **(E)** was determined by student *t*-test: $*P < 0.05$ and $**P < 0.01$.

Figure 3. Enzyme activities of AtPTPN and ZmPTPN.

(A) and **(E)** Substrate specificities of AtPTPN **(A)** and ZmPTPN **(E)** identified by the enzymatic substrate screening.

(B) and **(F)** Effects of temperature on AtPTPN **(B)** and ZmPTPN **(F)** activities in hydrolyzing GMP and dGMP.

(C) and **(G)** Effects of pH on AtPTPN **(C)** and ZmPTPN **(G)** activities in hydrolyzing GMP and dGMP.

(D) and **(H)** Effects of different divalent metal ions on enzymatic activities of AtPTPN **(D)** and ZmPTPN **(H)**. Various divalent metal ions (Ca^{2+}, Mg^{2+}, Mn^{2+}, Cu^{2+}) at different concentrations were added to the reaction mixtures. GMP was used as the substrate for both enzymes. Values represent means ± SD (n=3) from three replicates for all panels.

Figure 4. *AtPTPN* regulated AsA biosynthesis.

Journal Pre-proof

(A) A brief summary of the Smirnoff-Wheeler pathway. VTC1: mannose-1-P guanylyltransferase; GME: GDP mannose epimerase; VTC2/5: GDP-L-Galactosephosphorylase; VTC4: L-Galactose-1- phosphatase.

(B) AsA contents in 5-week-old wild type and *Atptpn-1* mutant plants with or without drought stresses (stopped watering for 12 days). Bars represent means ± SD of three replicates. DW, dry weight.

(C) Concentration of Pi in leaf tissues of WT and *Atptpn-1* mutant plants. 3 weeks seedlings were used for measurement. Error bars indicate SD (n=3). FW, fresh weight.

(D) Expression analyses of genes encoding key AsA biosynthetic enzymes, including *VTC1*, *VTC2*, *VTC4* and *VTC5,* in 5-week-old wild type and *Atptpn-1* mutants grown in the soil with or without drought stresses (stopped watering for 10 days). Bars represent means ± SD of three replicates.

(E) *VTC2* Expression levels in *VTC2*/C (#3, #7) and *VTC2*/*p* (#6, #29) transgenic lines.

(F) AsA contents in *VTC2*/C (#3, #7) and *VTC2*/*p* (#6, #29) transgenic lines. Four-week-old plants were used in **(E)** and **(F)**. Bars represent means ±SD of three replicates.

(G) Drought-tolerance phenotypes and survival rates of soil-grown *VTC2*/C (#3, #7) and *VTC2*/*p* (#6, #29) transgenic lines. Three-week-old plants were dehydrated for 13 days and then rehydrated for 3 days before phenotyping. Values represent means±SD obtained from three replicates with 50 plants each replicate. Statistical significance in panels **(B)** to **(G)** was determined by student *t*-test: $*P < 0.05$ and $**P < 0.01$.

Figure 5. The interaction between AtHSFA6a and *AtPTPN* promoter.

(A) A schematic diagram of the *AtPTPN* promoter region. The promoter was subdivided into 4 fragments designated P1, P2, P3 and P4, respectively. A heat stress element (HSE) was identified in P4 (red box indicated). The mutation of this HSE was indicated as HSEmu.

(B) and **(C)** Yeast one hybrid assays showed the interaction of HSFA6a with the P4 promoter fragment **(B)**, 3-AT was used to suppress background growth in the

experiment **(C)**. EV, empty vector. TFx, a transcription factor used as a control that shows no binding to the P4 promoter. *SAL1* promoter (SAL1p) is a negative control not bound by HSFA6a.

(D) EMSA showing HSFA6a binding to the P4 HSE motif, but not HSEmu sequence. The position of the HSFA6a-DNA complex is marked by a brace. dI-dC was added to the reactions unless indicated with ☆ (dI-dC was not added).

(E) Luciferase assays showing the activated expression of P4-driven reporter by HSFA6a in Arabidopsis protoplasts. EV, empty vector. Bars represent means ± SD of three replicates.

(F) Chip-qPCR analyses showing the binding of HSA6a to the DNA fragment with HSE in *AtPTPN* P4 promoter. The primers used in qPCR after chip are indicated as arrows (1)-(6) on the top of the panel. *SAL1* promoter (SAL1p) is a negative control not bound by HSFA6a. Statistical significance was determined by student *t*-test: $*P < 0.05$.

Figure 6. Genetic interactions between *HSFA6a* and *AtPTPN* in response to ABA and drought stresses.

(A) The *HSFA6a* expression levels in Col-0, two independent *HSFA6a-OE/*Col-0 (*HSFA6a*-OE/C) lines (#12, #17) and two independent *HSFA6a-OE/ptpn* (*HSFA6a*-OE/p) lines (#11, #22). Two-week-old transgenic and wild type plants were used in these expression assays. Bars are the means±SD of three replicates.

(B) The *AtPTPN* expression levels in Col-0, *HSFA6a*-OE/C (#12, #17) plants with or without drought stresses. Two-week-old transgenic and wild-type plants were dehydrated on dry filter paper, shoots were sampled at 0 and 1h for expression assays. Bars are the means±SD of three replicates.

(C) and **(D)** The cotyledon phenotypes **(C)** and the percentages of cotyledon greening **(D)** of wild-type, *HSFA6a*-OE/C (#12, #17), *HSFA6a*-OE/p (#11, #22) and *ptpn* in response to various concentrations of ABA. Col-0, *HSFA6a-OE/C* and *HSFA6a-OE/p* and *ptpn* seedlings were grown on MS plates with 0, 0.5, 0.75, 1.0 μM ABA for 5 days before phenotyping. Values represent means±SD (n>150) from three biological

replicates.

(E) and **(F)** Drought-tolerance phenotypes **(E)** and survival rates of wild-type, *HSFA6a-OE/C* and *HSFA6a-OE/p* **(F)** plants after drought treatments. Plants were grown in soil side-by-side. Three-week-old plants were dehydrated for 12, 14 or 16 days as indicated and then rehydrated for three days before phenotyping. Bars are the means±SD (n=30) of three replicates in **(F)**.

Statistical significance was determined by student *t* test: *P < 0.05, **P < 0.01.

Figure 7. A Working Model of AtPTPN.

In this model, AtPTPN functions in the nexus of ABA signaling and AsA biosynthesis pathways in plant drought tolerance. Drought enhances the ABA signaling, which in turn phosphorylates and activates the ABF transcription factors (TF). The active ABF TFs promotes *HSFA6a* expression levels via binding to the ABRE of *HSFA6a* promoter. HSFA6a in turn enhances *AtPTPN* expression levels via binding to the HSE in the *AtPTPN* promoter. AtPTPN hydrolyzes GDP/GMP/dGMP/IMP/dIMP to promote the endogenous Pi contents, which enhances the AsA production and facilitates plant drought tolerance.

Journal Pre-proof

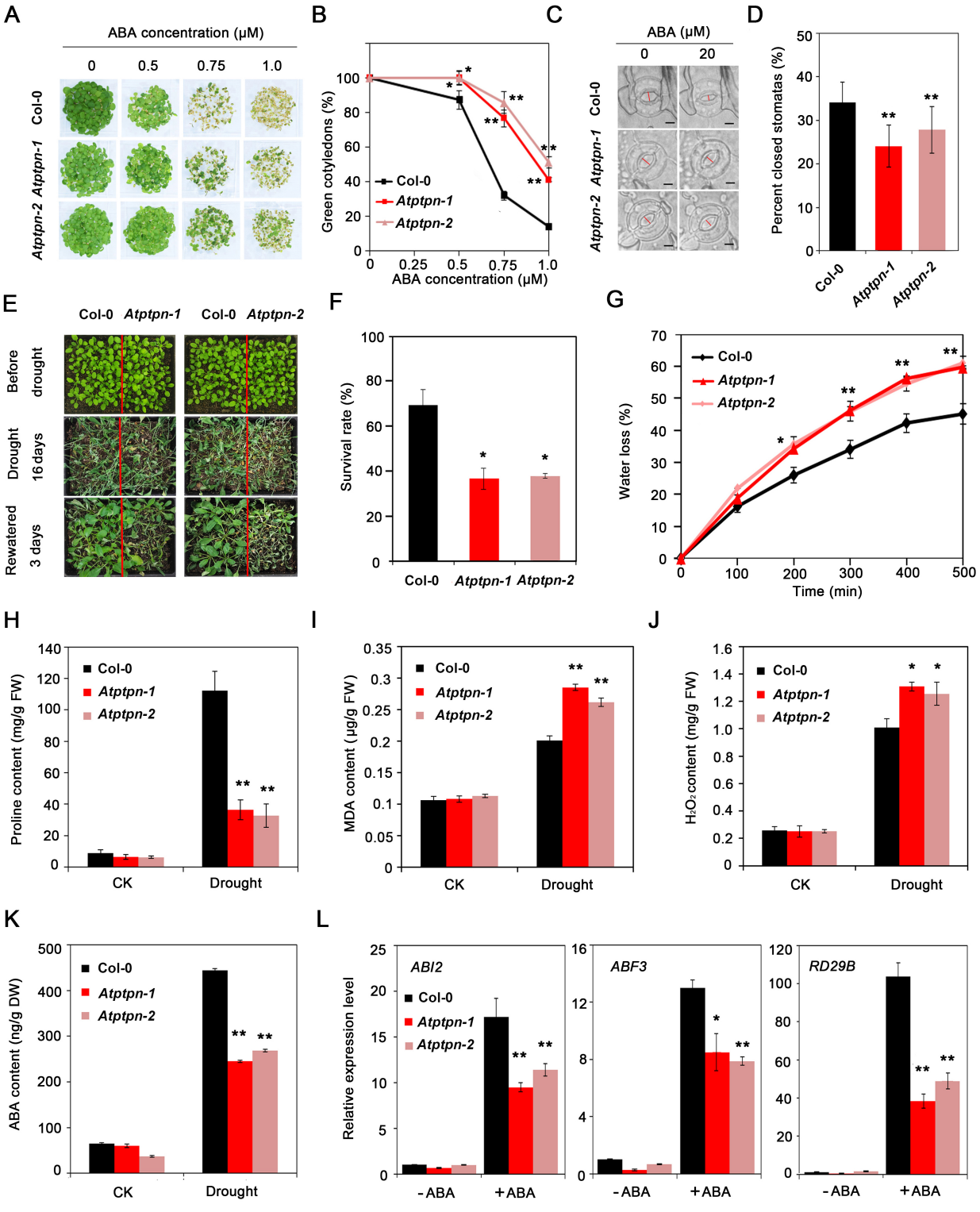
A
ABA concentration (μM)
0
0.5
0.75
1.0
Col-0
Atptpn-1
Atptpn-2
B
Green cotyledons (%)
ABA concentration (μM)
Col-0
Atptpn-1
Atptpn-2
C
ABA (μM)
0
20
D
Percent closed stomatas (%)
E
Col-0
Atptpn-1
Atptpn-2
Before drought
Drought 16 days
Rewatered 3 days
F
Survival rate (%)
G
Water loss (%)
Time (min)
H
Proline content (mg/g FW)
CK
Drought
I
MDA content (μg/g FW)
J
H2O2 content (mg/g FW)
K
ABA content (ng/g DW)
L
Relative expression level
ABI2
ABF3
RD29B
-ABA
+ABA

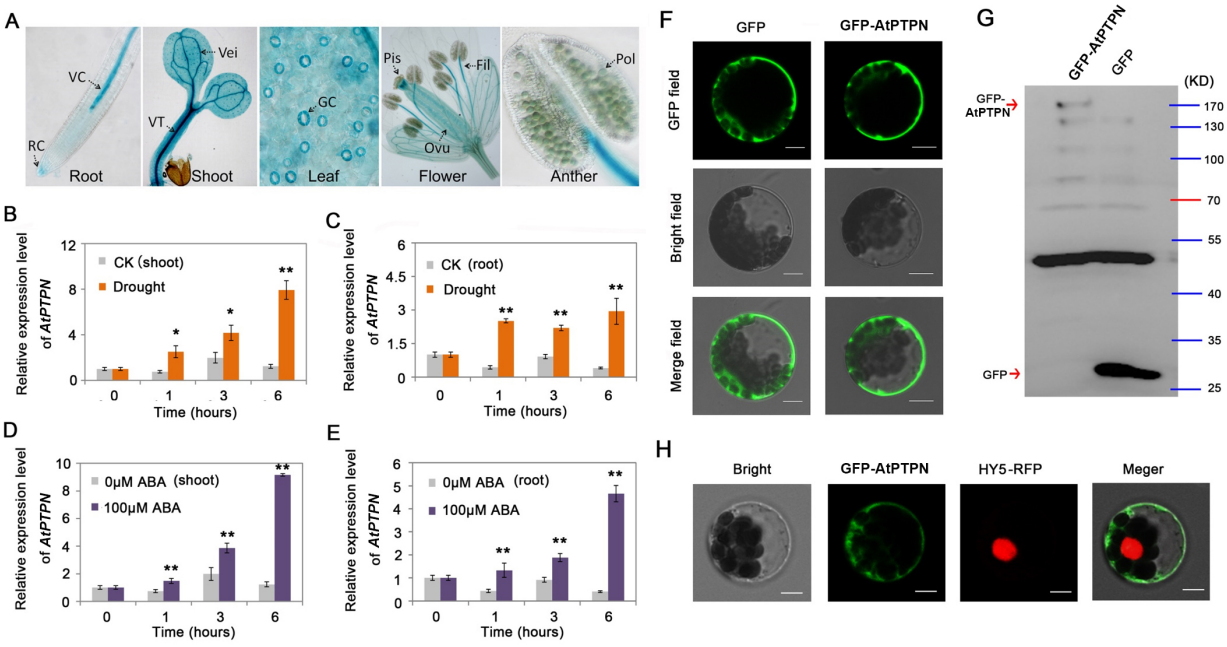

Journal Pre-proof

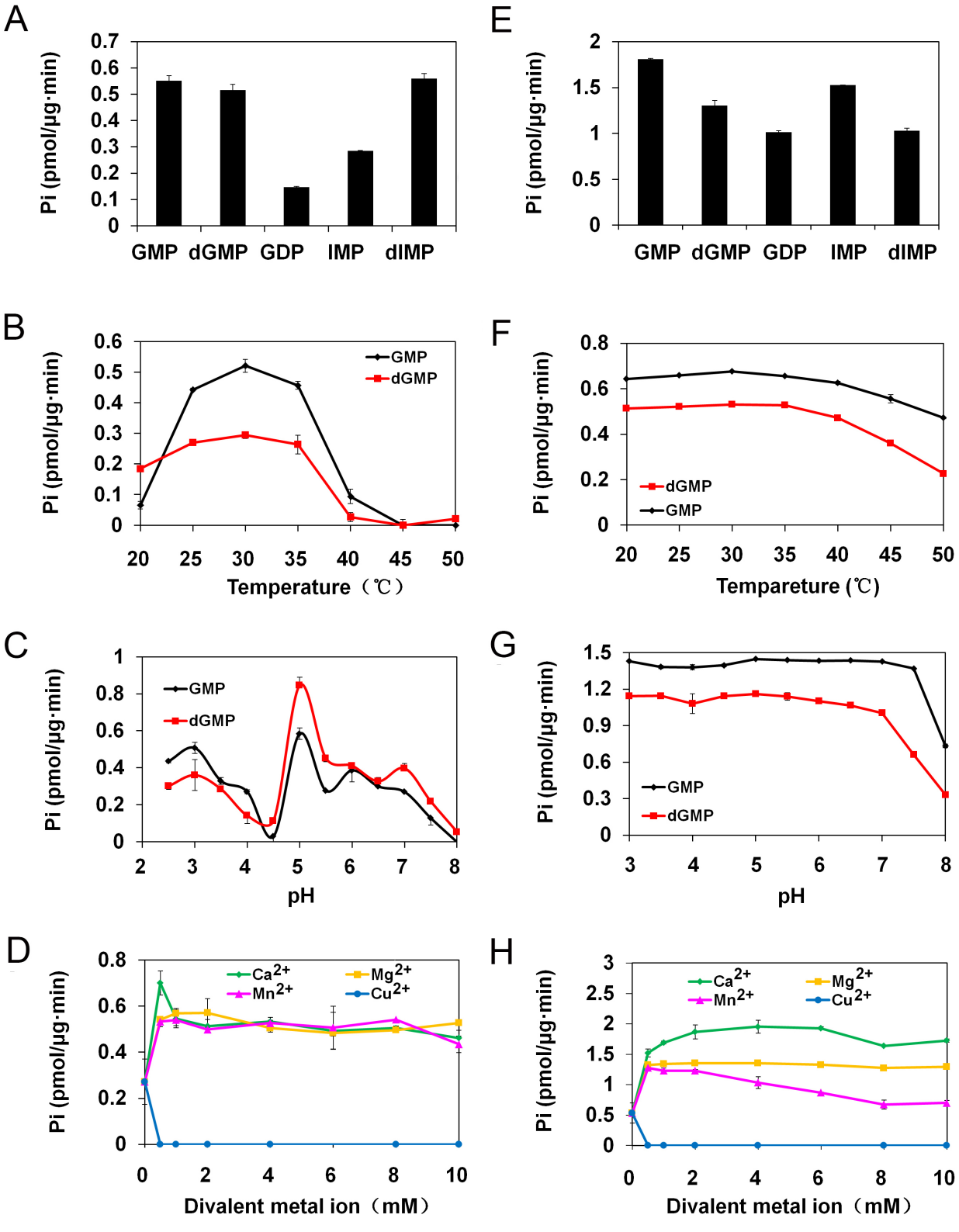
A
Pi (pmol/μg·min)
0.7
0.6
0.5
0.4
0.3
0.2
0.1
0
GMP dGMP GDP IMP dIMP
E
Pi (pmol/μg·min)
2
1.5
1
0.5
0
GMP dGMP GDP IMP dIMP
B
Pi (pmol/μg·min)
GMP
dGMP
0.6
0.5
0.4
0.3
0.2
0.1
0
20 25 30 35 40 45 50
Temperature（℃）
F
Pi (pmol/μg·min)
0.8
0.6
0.4
0.2
0
dGMP
GMP
20 25 30 35 40 45 50
Tempareture (℃)
C
Pi (pmol/μg·min)
GMP
dGMP
1
0.8
0.6
0.4
0.2
0
2 3 4 5 6 7 8
pH
G
Pi (pmol/μg·min)
1.5
1.2
0.9
0.6
0.3
0
GMP
dGMP
3 4 5 6 7 8
pH
D
Pi (pmol/μg·min)
Ca2+
Mn2+
Mg2+
Cu2+
0.8
0.6
0.4
0.2
0
0 2 4 6 8 10
Divalent metal ion（mM）
H
Pi (pmol/μg·min)
Ca2+
Mn2+
Mg2+
Cu2+
3
2.5
2
1.5
1
0.5
0
0 2 4 6 8 10
Divalent metal ion（mM）

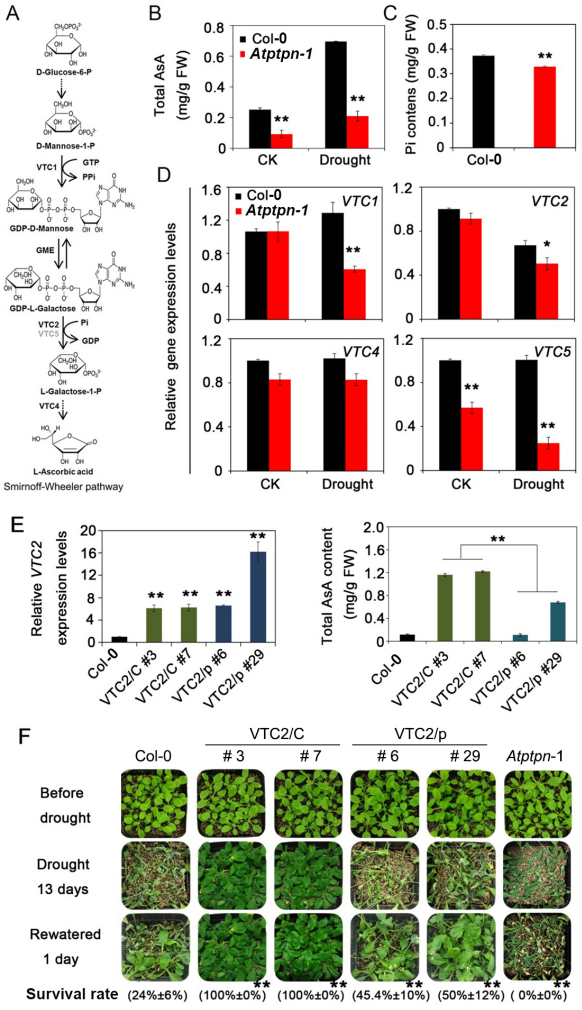

Journal Pre-proof

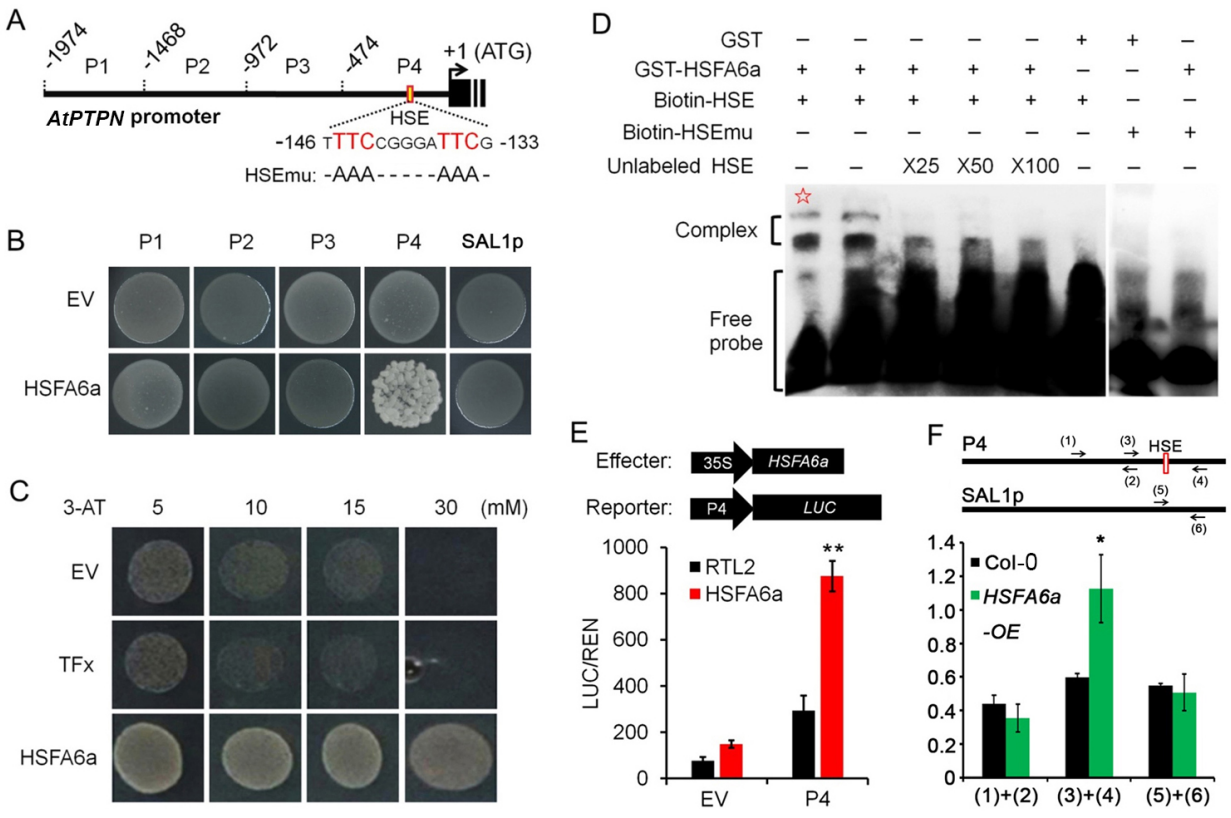
A
-1974
P1
-1468
P2
-972
P3
-474
P4
+1 (ATG)
AtPTPN promoter
HSE
-146 TTTCCGGGATTCG -133
HSEmu: -AAA-----AAA-
B
P1
P2
P3
P4
SAL1p
EV
HSFA6a
C
3-AT
5
10
15
30
(mM)
EV
TFx
HSFA6a
D
GST
GST-HSFA6a
Biotin-HSE
Biotin-HSEmu
Unlabeled HSE
X25
X50
X100
Complex
Free probe
E
Effecter:
35S
HSFA6a
Reporter:
P4
LUC
RTL2
HSFA6a
LUC/REN
1000
800
600
400
200
0
EV
P4
F
P4
(1)
(2)
(3)
(4)
(5)
(6)
HSE
SAL1p
Col-0
HSFA6a
-OE
1.4
1.2
1.0
0.8
0.6
0.4
0.2
0
(1)+(2)
(3)+(4)
(5)+(6)

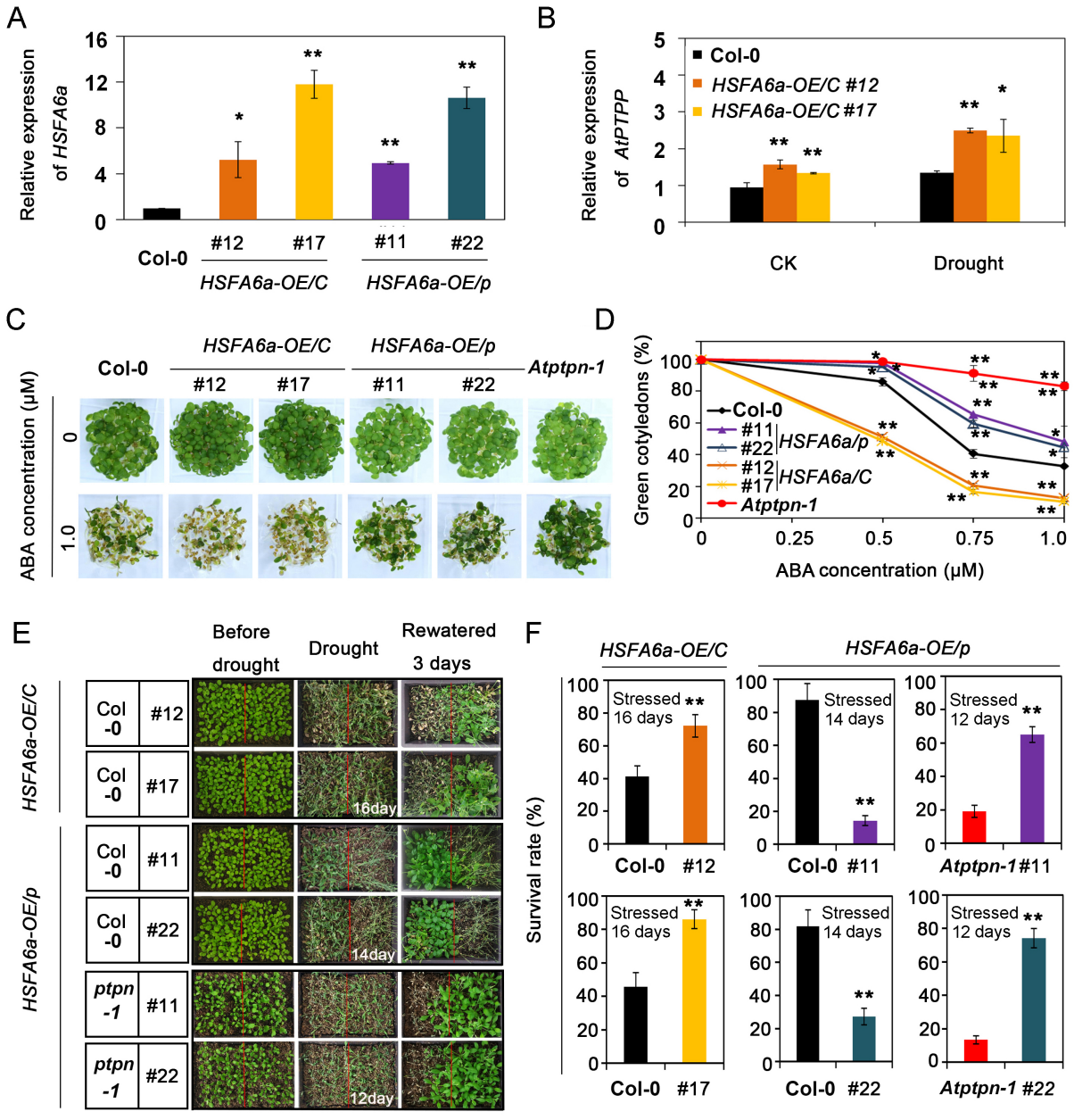
A
Relative expression of HSFA6a
16
12
8
4
0
Col-0
#12
#17
#11
#22
HSFA6a-OE/C
HSFA6a-OE/p
B
Relative expression of AtPTPP
5
4
3
2
1
0
Col-0
HSFA6a-OE/C #12
HSFA6a-OE/C #17
CK
Drought
C
Col-0
HSFA6a-OE/C
HSFA6a-OE/p
Atptpn-1
#12
#17
#11
#22
ABA concentration (μM)
0
1.0
D
Green cotyledons (%)
100
80
60
40
20
0
Col-0
#11
#22
HSFA6a/p
#12
#17
HSFA6a/C
Atptpn-1
0
0.25
0.5
0.75
1.0
ABA concentration (μM)
E
Before drought
Drought
Rewatered 3 days
HSFA6a-OE/C
HSFA6a-OE/p
Col -0
#12
Col -0
#17
16day
Col -0
#11
Col -0
#22
14day
ptpn -1
#11
ptpn -1
#22
12day
F
HSFA6a-OE/C
HSFA6a-OE/p
Survival rate (%)
Stressed 16 days
Stressed 14 days
Stressed 12 days
Col-0 #12
Col-0 #11
Atptpn-1#11
Col-0 #17
Col-0 #22
Atptpn-1 #22

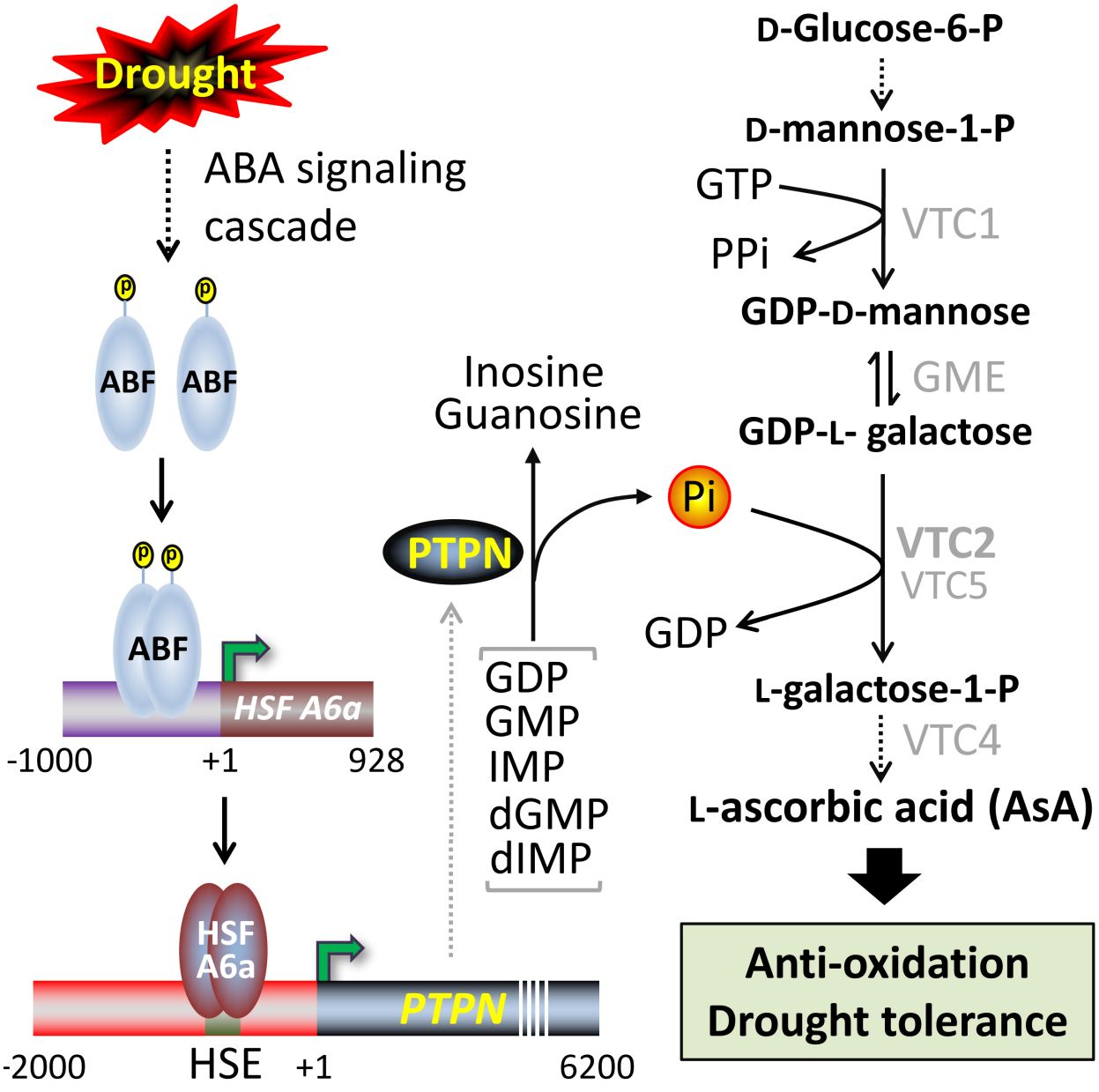
Drought
ABA signaling cascade
ABF
ABF
ABF
HSF A6a
-1000
+1
928
HSF A6a
PTPN
-2000
HSE
+1
6200
Inosine
Guanosine
PTPN
GDP
GMP
IMP
dGMP
dIMP
D-Glucose-6-P
D-mannose-1-P
GTP
PPi
VTC1
GDP-D-mannose
GME
GDP-L- galactose
Pi
VTC2
VTC5
GDP
L-galactose-1-P
VTC4
L-ascorbic acid (AsA)
Anti-oxidation
Drought tolerance